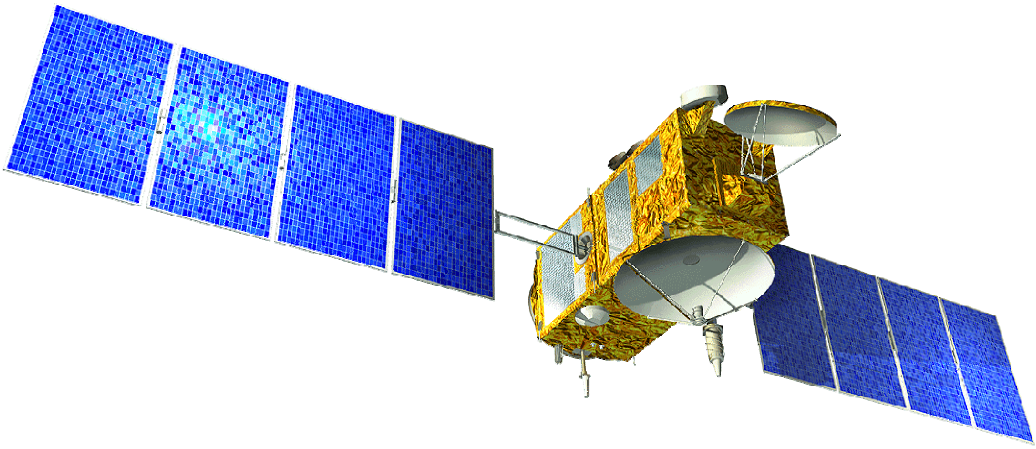

Jason-1 Products Handbook

References:
CNES : SALP-MU-M5-OP-13184-CN
JPL : JPL D-21352
Issue: 5 rev 1
Date: April 4th, 2016

Chronology Issues:

Issue:	Date:	Modifications	Visa
2rev0	14 April 2003	Initial release to users In line with products named JA1_GDR_2Pa generated since the beginning of the mission	N Picot
2rev1	October 2004	Modification on 20Hz field management. Implemented on IGDR data starting with cycle 102 and on GDR/SGDR data starting with cycle 91. No impact on the 1 Hz data.	N. Picot
3rev0	07 December 2005	Accounting for all evolutions included in GDR v2 version. In line with products named JA1_GDR_2Pb Implemented on IGDR data starting on October, 24th 2005 (i.e. first day of cycle 140) and on GDR/SGDR data starting on cycle 136 (for the routine processing)	N. Picot S. Desai
4rev0	June 2008	Accounting for all evolutions included in GDR_C version. Accounting for evolution regarding mog2D correction inside IGDR products. In line with products named JA1_GDR_2Pc and JA1_IGD_2Pc Implemented on IGDR data starting on June, 17th (ie JA1_IGD_2PcP237_121) and on GDR/SGDR data starting on cycle 233 (for the routine processing).	N. Picot S. Desai J. Hausman
4rev1	September 2008	POE standard modification (Time variable Gravity terms of order > 1 removed) Correction of GDR_C version scope (instrumental corrections have been updated) In line with products named JA1_GDR_2Pc and JA1_IGD_2Pc.	N. Picot S. Desai
4rev2	June 2012	Evolutions to take into account new Jason-1 new geodetic orbit: - New orbit characteristics - Modification of cycles/tracks numbering - POD standard modification (GDR-D) - New Mean Sea Surface : CNES-CLS-2011	E. Bronner
5rev0	September 2015	- Update to take into account Jason-1 reprocessing of GDR products in version 'e' (Change request SALP-FT-10180) - New template of products handbook document to be in line with Jason-2 and	E. Bronner N. Picot S. Desai J. Hausman

Chronology Issues:			
Issue:	Date:	Modifications	Visa
		Jason-3 mission.	
5rev1	April 2016	Update to take into account corrections of reprocessing tool and auxiliary data.	E. Bronner N. Picot L. Carrère S. Desai J-D. Desjonquères N. Tran

People involved in this issue:		
Written by (*):		Date :
E. BRONNER	CNES	On behalf of the team
N. PICOT	CNES	4 April 2016
J-D. DESJONQUERES	CNES	Bronner
S. DESAI	NASA/JPL	
J. HAUSMAN	NASA/JPL/PODAAC	
L. CARRERE	CLS	
N. TRAN	CLS	

List of tables and figures

List of tables:

List of figures:

Applicable documents / reference documents

AD 1 : **Jason-1 System Requirements**
TP2-SB-J0-100-CNES

AD 2 : **Jason-1 Science and Operational Requirements**
TP2-SB-J0-102-CNES

AD 3 : ADAS, « Algorithm Definition Accuracy Specification Vol 1 : **Jason real time processing** » SMM-ST-M2-EA-11002-CN

AD 4 : ADAS, « Algorithm Definition Accuracy Specification Vol 2 : **CMA altimeter level 1B processing** » SMM-ST-M2-EA-11003-CN

AD 5 : ADAS, « Algorithm Definition Accuracy Specification Vol 3 : **CMA radiometer level 1B processing** » SMM-ST-M2-EA-11004-CN

AD 6 : ADAS, « Algorithm Definition Accuracy Specification Vol 4 : **CMA altimeter level 2 processing** » SMM-ST-M2-EA-11005-CN

AD 7 : ADAS, « Algorithm Definition Accuracy Specification Vol 5 : **CMA radiometer level 2 processing** » SMM-ST-M2-EA-11006-CN

AD 8 : ADAS, « Algorithm Definition Accuracy Specification Vol 6 : **CMA altimeter / radiometer verification processing** » SMM-ST-M2-EA-11007-CN

AD 9 : ADAS, « Algorithm Definition Accuracy Specification Vol 7 : **Near real time control processing** » SMM-ST-M2-EA-11008-CN

AD 10 : ADAS, « Algorithm Definition Accuracy Specification Vol 8 : **Off line control processing** » SMM-ST-M2-EA-11009-CN

AD 11 : ADAS, « Algorithm Definition Accuracy Specification Vol 9 : **CMA mechanisms** » SMM-ST-M2-EA-11010-CN

AD 12 : ADAS, « Algorithm Definition Accuracy Specification Vol 11 : **Visualisation processing** » SMM-ST-M2-EA-11012-CN

AD 13 : ADAS, « Algorithm Definition Accuracy Specification Vol 12 : **CMA/DORIS** » **ionospheric processing** » SMM-SP-M2-EA-11013-CN

RD 1 : **TOPEX/POSEIDON Project, 1992, "GDR-T User's Handbook"**
PD 633-721, JPL D-8944, October 18, 1993

RD 2 : **AVISO and PODAAC User Handbook - IGDR and GDR Jason Products**
SMM-MU-M5-OP-13184-CN (AVISO), JPL D-21352 (PODAAC)

RD 3 : **OSTM/Jason-2 Products Handbook**
SALP-MU-M-OP-15815-CN

RD 4 : **Rain Flag Modification for Version B Jason GDRs**
Doc. Techni/ DOPS/LOS, 2006-01

Contents

1. Introduction

Jason-1 is a follow-on mission to the highly successful TOPEX/POSEIDON (T/P) mission. It was launched on 7 December 2001 and decommissioned on 21 June 2013. The satellite is named after the leader of the Argonauts' famous quest to recover the Golden Fleece. The Jason-1 mission is jointly conducted by the French Space Agency, "*Centre National d'Etudes Spatiales*" (CNES) and the United States National Aeronautics and Space Administration (NASA).

1.1. Overview of the Jason-1 product family

The purpose of this document is to assist users of the Jason-1 version E reprocessed products that have been generated after the conclusion of the mission. Reprocessed products only include the fully validated Geophysical Data Record (GDR), and supersede all prior versions and product families from the Jason-1 mission.

During mission operations, there were three product families (Operational Sensor Data Record: OSDR, Interim Geophysical Data Record: IGDR, and Geophysical Data Record : GDR) that are described in previous versions of this user handbook. The OSDR was a non-validated near-real-time (3-hour latency) product aimed towards wind/wave users. The IGDR and GDR were identical except for the following differences regarding auxiliary data used in the processing. These differences resulted from the product latencies of 2-3 days for the IGDR and 30 days for the GDR.

Auxiliary Data	Impacted Parameter	OSDR	IGDR	GDR
Orbit	Satellite altitude, Doppler correction, …	DORIS Navigator	Preliminary (MOE using DORIS data)	Precise (POE using DORIS and/or Laser and/or GPS data)
Meteo Fields	Dry/wet tropospheric corrections, U/V wind vector, Surface pressure, Inverted barometer correction, …	Not available	Restituted	
Pole Location	Pole tide height	Not available	Predicted	Restituted
Mog2D	HF ocean dealiasing correction	Not available	Preliminary	Precise
GIM	Ionosphere correction	Not available	Available	

Table 1 : Differences between Auxiliary Data for O/I/GDR Products

GDR products, unlike OSDR and IGDR products, are fully validated products.

1.1.1. Product contents

The version E GDR products from this mission comprise three types of files in NetCDF format, with increasing size and complexity:

1. a reduced (R) 1 Hz subset of the full dataset in NetCDF format (GDR-SSHA);
2. the native (N) NetCDF formatted datasets (GDRs) which contain 1Hz records as well as 20 Hz high-rate values;
3. an expert sensor (S) product containing the full radar-echo waveforms in NetCDF format (S-GDR).

The format of these products closely follows that from the follow-on Jason-2 mission. All files contain sea surface height, ocean surface wind speed, significant wave height information and all required corrections. The files differ in the amount and type of auxiliary data included but the product format is the same.

1.1.2. Filename conventions

The version E GDR product names are based on the following convention:

JA1_GP<N/R/S>_2P<v>P<ccc>_<ppp>_<yyyymmdd_hhnnss>_<yyyymmdd_hhnnss>.nc

With :

<N/R/S> : product type (N : native, R: reduced, S : sensor)
<v> : product version (set to 'e' for the current delivery of Jason-1 reprocessed products)
<ccc>: cycle number of 1st product record
<ppp> : pass number of 1st product record (1-254)
<yyyymmdd_hhnnss> : date of 1st product record
<yyyymmdd_hhnnss> : date of last product record

Offline GDR products:

GDR:	JA1_GPN_2PvPccc_ppp_yyyymmdd_hhnnss_yyyymmdd_hhnnss.nc
GDR-SSHA:	JA1_GPR_2PvPccc_ppp_yyyymmdd_hhnnss_yyyymmdd_hhnnss.nc
S-GDR:	JA1_GPS_2PvPccc_ppp_yyyymmdd_hhnnss_yyyymmdd_hhnnss.nc

Binary formats and contents of the Jason-1 products during mission operations (versions a, b, c) are described in previous versions of "Jason-1 product handbook" and "Jason-1 user products".

1.2. Handbook Overview

This is a combination of a guide to data use and a reference handbook, so not all sections will be needed by all readers.

Section 1 provides information on product evolution history

Section 2 provides background information about the GDR and this document

Section 3 is an overview of the Jason-1 mission

Section 4 is an introduction to using the Jason-1 data

Section 5 is an introduction to the Jason-1 altimeter algorithms

Section 6 provides a description of the content and format of the Jason-1 GDRs

Appendix A contains references

Appendix B contains acronyms

Appendix C describes how to order information or data from CNES and NASA, and lists related Web sites.

1.3. Document reference and contributors

When referencing this document, please use the following citation:

"Jason-1 Products Handbook",

CNES (AVISO+) :	**SALP-MU-M5-OP-13184-CN**
JPL (PODAAC) :	**JPL D-21354**

This document is based on "Jason-2 products handbook" and "AVISO and PODAAC User Handbook. IGDR and GDR Jason Products".

All contributors are: N. Picot, S. Desai, P. Vincent, E. Bronner, K. Case, P. Callahan, R. Benada, and V. Zlotnicki, J. Lambin, F. Boy, T. Guinle, L. Carrère, J.P. Dumont, V. Rosmorduc, H. Bonekamp, J. Figa, J. Lillibridge, R. Scharroo, A. Couhert.

1.4. Conventions

1.4.1. Vocabulary

1.4.1.1. Altimetric distances

In order to reduce confusion in discussing altimeter measurements and corrections, the following terms are used in this document as defined below:

- **Distance** and **Length** are general terms with no special meaning in this document
- **Range** is the distance from the satellite to the surface of the Earth, as measured by the altimeter. Thus, the altimeter measurement is referred to as "range" or "altimeter range," not height
- **Altitude** is the distance of the satellite or altimeter above a reference point. The reference point used is the reference ellipsoid. This distance is computed from the satellite ephemeris data
- **Height** is the distance of the sea surface above the reference ellipsoid. The sea surface height is the difference of the altimeter range from the satellite altitude above the reference ellipsoid

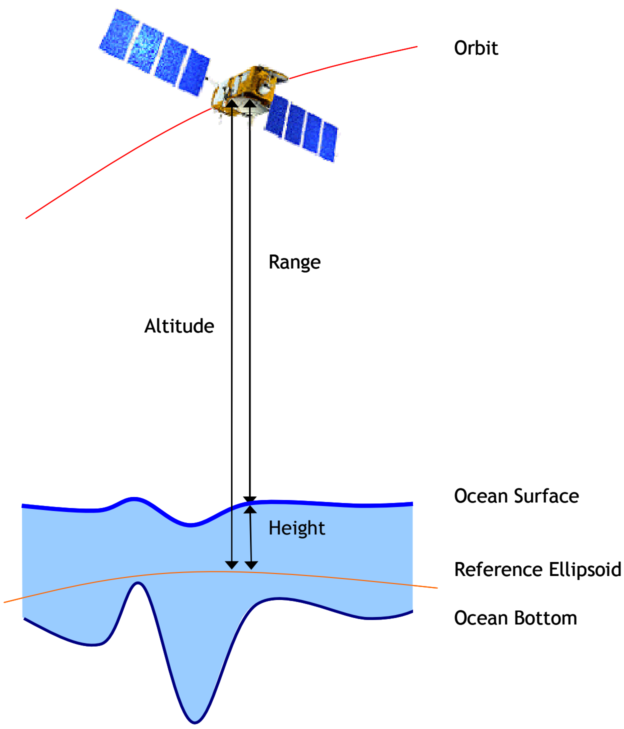

Figure 1 : Altimetric distances – Altitude, Range and Height

1.4.1.2. Orbits, Revolutions, Passes, and Repeat Cycles

An **Orbit** is one circuit of the earth by the satellite as measured from one ascending node crossing to the next. An ascending node occurs when the sub satellite point crosses the earth's equator going from south to north. A **Revolution** (REV) is synonymous with orbit.

The OSDR data were organized into files ("segments") which corresponded to the amount of data dumped over an Earth terminal (typically 2 hour-data sets).

The (I)GDR data is organized into pass files in order to avoid having data boundaries in the middle of the oceans, as would happen if the data were organized by orbit. A **Pass** is half a revolution of the earth by the satellite from extreme latitude to the opposite extreme latitude.

For Jason-1, an **Ascending Pass** begins at the latitude -66.15 deg and ends at +66.15 deg. A **Descending Pass** is the opposite (+66.15 deg to -66.15 deg).

On the **repetitive orbit**, the passes are numbered from 1 to 254 representing a full repeat cycle of the Jason-1 ground track. Ascending passes are odd numbered and descending passes are even numbered. After one repeat cycle of 254 passes, Jason-1 revisits the same ground-track within a margin of ±1 km. That means that every location along the Jason-1 ground-track is measured every approximately 9.9 days.

On the **geodetic orbit** (from May, 2012), the passes are numbered from 1 to 280 (i.e. sub-cycle of 10.9 days).

1.4.1.3. Reference Ellipsoid

The **Reference Ellipsoid** is the first-order definition of the non-spherical shape of the Earth as an ellipsoid of revolution with equatorial radius of 6378.1363 kilometers and a flattening coefficient of 1/298.257 (same reference ellipsoid as used by the T/P missions).

1.4.2. Correction Conventions

All environmental and instrument corrections are computed so that they should be added to the quantity which they correct. That is, a correction is applied to a measured value by

Corrected Quantity = Measured Value + Correction

This means that a correction to the altimeter range for an effect that lengthens the apparent signal path (e.g., wet troposphere correction) is computed as a negative number. Adding this negative number to the uncorrected (measured) range reduces the range from its original value toward the correct value. Example: Corrected Range = Measured Range + Range Correction.

1.4.3. Time Convention

For Jason-1 products release “GDR-E”, measurement time tags are UTC and referenced to **January 1, 2000 00:00:00.00**. Note that for Jason-1 products before release “GDR-E”, measurement time tags were UTC and referenced to **January 1, 1958 00:00:00.00**, sometimes abbreviated UTC58.

A UTC leap second can occur on June 30 or December 31 of any year. The leap second is a sixty-first second introduced in the last minute of the day. Thus the UTC values (minutes:seconds) appear as: 59:58 ; 59:59 ; 59:60 ; 00:00 ; 00:01.

1.4.4. Unit Convention

All distances and distance corrections are reported in tenths of millimeters (10^{-1} mm).

1.4.5. Flagging and Editing

In general, flagging consists of three parts: instrument flags (on/off), telemetry flags (preliminary flagging and editing) and data quality flags (geophysical processing flags).

Instrument flags provide information about the state of the various instruments on the satellite.

Telemetry flags are first based on instrument modes and checking of telemetry data quality. Only severely corrupted data are not processed (i.e. data that cannot be correctly read on ground). Flag setting is designed to get a maximum amount of data into the “Sensor Data Records” (part of the SGDR data sets). Science data are processed only when the altimeter is in tracking mode.

Quality flags are determined from various statistical checks on the residuals after smoothing or fitting through the data themselves. These flags are set if gaps in the data are detected, or residuals have exceeded predetermined thresholds, or if the gradients of the data exceed predetermined thresholds.

2. Jason-1 Mission Overview

2.1. Background

Jason-1 is jointly conducted by the French Space Agency, "*Centre National d'Etudes Spatiales*" (CNES), and the United States' National Aeronautics and Space Administration (NASA) for studying the global circulation from space. The mission used the technique of satellite altimetry to make precise and accurate observations of sea level for several years. Jason-1 was launched on 7 December 2001 and was decommissioned on 21 June 2013.

2.2. Jason-1 Mission

Jason-1 was a follow-on mission to the highly successful TOPEX/POSEIDON (T/P) mission. The main goal of this mission was to measure the sea surface topography at least at the same performance level of T/P. This provided an extended continuous time series of high-accuracy measurements of the ocean topography from which scientists can determine the general circulation of the ocean and understand its role in the Earth's climate. In addition to the primary Jason-1 IGDR and GDR data products provided with a 2-3 and 30 day latency, respectively, Jason-1 also supported the preparation of operational ocean services by providing a non-validated near-real-time (3 hour latency) Jason-1 data product, the Operational Sensor Data Record (OSDR). Jason-1 was the first in a twenty-year series of satellites to take over from T/P, marking the start of operational satellite altimetry.

The Jason-1 mission supports new research programs such as the Climate Variability and Predictability program (CLIVAR) and the Global Ocean Data Assimilation Experiment (GODAE).

2.3. Jason-1 Requirements

The major elements of the mission include a satellite carrying an altimetric system for measuring the height of the satellite above the sea surface; a precision orbit determination system for referring the altimetric measurements to geodetic coordinates; a data analysis and distribution system for processing the satellite data, verifying their accuracy, and making them available to the scientific community; and a Principal Investigator program for scientific studies based on the satellite observations.

The Jason-1 mission was designed in a way that allows an optimum continuation of the T/P scientific mission. This means that the error budget and orbit characteristics (repeat period, inclination, altitude) of Jason-1 were identical to those of T/P. To ensure that science and mission goals were accomplished by the Jason-1 mission, the following requirements were established.

2.3.1. Accuracy of Sea-level Measurements

Requirements for the Jason-1 (I)GDR are derived directly from the post-launch T/P error budget, with the Jason-1 system required to be at least as good as the T/P system. Each measurement of sea level shall have an accuracy of ±4.2 cm for the GDR products and 5.2 cm for the IGDR (1 standard deviation) over 1 second averages for typical oceanic conditions of 2 m significant wave height and 11dB sigma-naught. This error budget includes the altimeter noise, uncertainties in corrections of atmospheric path delays, sea-state related biases, and orbit error.

The following table provides a summary of error budget at the end of the verification phase.

	IGDR (3 days)		GDR (30 days)	
	Spec	Performance	Spec	Performance
Altimeter noise (cm) (H1/3=2m, σ=11dB) 1Hz	*1.7*	1.6	*1.7*	1.6
Sea State Bias (%H1/3)	*1.2%*	1% *	*1.2%*	1% *
Ionosphere (cm)	*0.5***	0.5**	*0.5***	0.5**
Dry Tropo (cm)	*0.7*	0.7	*0.7*	0.7
Wet Tropo (cm)	*1.2*	1.2	*1.2*	1.2
Corrected Range (RSS, cm) (H1/3=2m, σ=11dB) 1Hz	*3.3*	3	*3.3*	3
Orbit (radial component) (cm)	*4*	2.5	*2.5*	1.5
Corrected Sea Surface Height (RSS,cm) (H1/3=2m, σ=11dB) 1 Hz	*5.2*	3.9	*4.2*	3.3
Wave Height H1/3 (m or %H1/3, whichever is greater)	*0.5 or 10%*	0.4 *** or 10%	*0.5 or 10%*	0.4 *** or 10%
Wind Speed (m/s)	*1.7*	1.5 ***	*1.7*	1.5 ***

* improvement studies in progress
** after filtering over 100 km
*** after bias calibration

Table 2 : Summary of error budget at the end of the verification phase

2.3.2. Sampling Strategy

Sea level shall be measured along a fixed grid of sub satellite tracks such that it is possible to investigate and minimize the spatial and temporal aliases of surface geostrophic currents and to minimize the influence of the geoid on measurements of the time-varying topography.

2.3.3. Tidal Aliases

Sea level shall be measured such that tidal signals are not aliased into semiannual, annual, or zero frequencies (which influences the calculation of the permanent circulation) or frequencies close to these.

2.3.4. Duration and coverage

Sea level shall be measured for a minimum of three years, with the potential to extend this period for an additional two years.

The Jason-1 satellite shall overfly the reference T/P ground tracks. The grid of sub satellite tracks shall extend in latitude at least as far south as the southern limit of the Drake Passage (62 deg) and the sub satellite tracks that comprise the grid will cross at sufficiently large angles that the two orthogonal components of surface slope can be determined with comparable accuracy.

3.2.5. Data Reduction and Distribution

A system to process and distribute data to the Principal Investigators shall be tested, documented, and in operation at the time of launch. A minimum of 95% of the oceanic data that could be acquired by the spacecraft shall be acquired with no systematic gaps, processed and made available for scientific investigations. The intent is to collect and process all data continuously. Small amounts of data could be lost during adjustments of the satellite's orbit, during tests of the altimeter's performance, and during various other such events.

2.4. Satellite Description

The 500 kg satellite consists of a multi-mission PROTEUS platform and a Jason-1 specific payload module. The platform provides all housekeeping functions including propulsion, electrical power, command and data handling, telecommunications, and attitude control. The payload module provides mechanical, electrical, thermal, and dynamical support to the Jason-1 instruments.

The Jason-1 payload (see Figure 2) included the following components:

- **An Altimeter (Poseidon-2)**, provided by CNES – the main mission instrument
- **A Microwave Radiometer (JMR),** provided by NASA – to correct the altimeter measurement for atmospheric range delays induced by water vapor
- **The radio positioning DORIS system**, provided by CNES – for precision orbit determination using dedicated ground stations
- **A Laser Reflector Array (LRA),** provided by NASA – to calibrate the orbit determination system
- **A Turbo Rogue Space Receiver (TRSR),** provided by NASA - to provide supplementary positioning data to DORIS in support of the POD function and to enhance and/or improve gravity field models

Figure 2 : Main components of the Jason-1 satellite

2.4.1. Satellite Characteristics

The main features of the Jason-1 satellite are summed up in the following table.

Satellite mass	500 kg
Satellite power	450 W
Platform mass	270 kg
Platform power	300 W
Payload mass	120 kg
Payload power	147 W
Altimeter mass	55 kg
Altimeter power	78 W
Launch Vehicle	Dual Delta II
Launch Site	Vandenberg Air Force Base (AFB)

Table 3 : Main features of the Jason-1 satellite

2.4.2. Sensors

The science and mission goals are carried out with a satellite carrying five science instruments, three from CNES and two from NASA.

2.4.2.1. Poseidon-2 Altimeter

The Poseidon-2 Dual-frequency Ku/C band Solid State Radar altimeter, operating at 13.575 GHz (Ku band) and 5.3 GHz (C band), is the primary sensor for the Jason-1 mission. The measurements made at the two frequencies are combined to obtain measurements of the altimeter range, wind speed, significant wave height, and the ionospheric correction. The Poseidon-2 package consists of dual redundant altimeter units each of which has low mass and low power consumption.

2.4.2.2. Jason-1 Microwave Radiometer (JMR)

The JMR measures the sea surface microwave brightness temperatures at three frequencies (18.7 GHz, 23.8 GHz and 34.0 GHz) to provide the total water vapor content in the troposphere along the altimeter beam. The 23.8 GHz channel is the primary channel for water-vapor measurement and is a redundant channel on the JMR. The 18.7 GHz channel provides a correction for wind-induced effects in the sea surface background emissions, and the 34.0 GHz channel provides a correction for cloud liquid water. The measurements are combined to obtain the error in the satellite range measurements caused by pulse delay due to the water vapor.

2.4.2.3. DORIS System

The Doppler Orbitography and Radiopositioning by Satellite (DORIS) Precise Orbit Determination (POD) system uses a two-channel, two-frequency (401.25 MHz and 2036.25 MHz) Doppler receiver on the satellite to observe the tracking signals from a network of approximately 50 ground transmitting beacons. It provides all-weather global tracking of the satellite for POD and a correction for the influence of the ionosphere on both the Doppler signal and altimeter signals. The DORIS on-board package includes the receiver itself, the ultra-stable oscillator, and an omni-directional antenna located on the nadir face of the satellite. It includes a dual beacon receiving capability and an on-board real time function (Détermination Immédiate d'Orbite par Doris Embarqué, or DIODE) to compute the orbit ephemeris with an accuracy of 30 cm (1 standard deviation).

2.4.2.4. Laser Reflector Array

The LRA is placed on the nadir face of the satellite and reflects signals from a network of 10 to 15 satellite laser tracking stations. It supports the Jason-1 Calibration and Validation function for POD.

2.4.2.5. Turbo Rogue Space Receiver

The TRSR is an advanced codeless sixteen-channel Global Positioning System (GPS) receiver developed by the Jet Propulsion Laboratory (JPL). The on-board package is comprised of dual redundant TRSR units and choke ring antennae. The GPS data are intended to provide supplementary positioning data in support of the POD function and/or to improve gravity field models.

2.4.3. Orbit

2.4.3.1. Repetitive Orbit (Dec. 2001 - May 2012)

The Jason-1 satellite will fly the same ground-track as the original T/P with a 254 pass, 10-day exact repeat cycle. The Jason-1 and T/P satellites were phased approximately 70 seconds apart during the calibration phase.

On August 15, 2002 (T/P cycle 365 pass 111) the T/P satellite began its “drift phase” by moving to a new orbit in preparation for the Tandem Mission. The drift phase lasted until September 16, 2002 ending with cycle 368, pass 171. Data for T/P cycle 368, pass 172 and later are on the final exact-repeat tandem mission ground track, which is interleaved with the original Jason-1 ground track, providing improved temporal and spatial coverage. Orbital characteristics and the equator crossing longitudes for the original ground track of Jason-1 are given below. Figure 3 is a plot of the ground track on a world map.

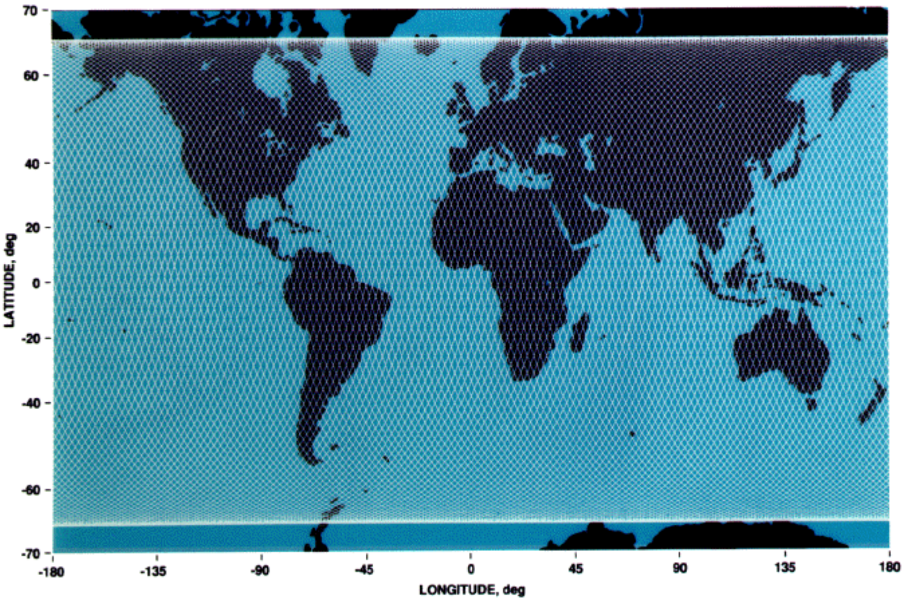

Figure 3 : T/P and Jason-1 ground track coverage every 10 days

A similar tandem mission between Jason-1 and Jason-2 became available after the launch of Jason-2 on June 20, 2008. In this case, Jason-1 and Jason-2 satellites were phased approximately 56 seconds apart on the same ground track during the Jason-2 calibration phase. Jason-1 started a drift phase on January 26, 2009 (Jason-1 repeat cycle 260) until it reached the interleaving tandem mission ground track, previously flown by T/P, on February 10, 2009 (Jason-1 repeat cycle 262).

The mean classical orbit elements are given in the table below:

Orbit element	Value
Semi-major axis	7,714.43 km
Eccentricity	0.000095
Inclination	66.04 deg
Argument of periapsis	90.0 deg
Inertial longitude of the ascending node	116.56 deg
Mean anomaly	253.13 deg

Table 4 : Mean classical orbit elements

The orbit auxiliary data are given in the table below:

Auxiliary Data	Values
Reference (Equatorial) altitude	1,336 km
Nodal period	6,745.72 sec
Repeat period	9.9156 days
Number of revolutions within a cycle	127
Equatorial cross-track separation	315 km
Ground track control band	$\pm$ 1 km (at equator)
Acute angle at Equator crossings	39.5 deg
Longitude of Equator crossing of pass 1	99.9249 deg
Inertial nodal rate	-2.08 deg/day
Orbital speed	7.2 km/s
Ground track speed	5.8 km/s

Table 5 : Orbit auxiliary data

This orbit overflies two verifications sites. The prime CNES verification site is located at Cape Senetosa on the island of Corsica (8° 48' E, 41° 34' N (ascending pass 85) (*Bonnefond et al.*, 2002). The prime NASA verification site is located on the Harvest oil platform near Pt. Conception, California (239° 19' E, 34° 28' N) (ascending pass 43) (*Haines et al.*, 2002).

A satellite orbit slowly decays due to air drag, and has long-period variability because of the inhomogeneous gravity field of Earth, solar radiation pressure, and smaller forces. Periodic maneuvers are required to keep the satellite in its orbit. The frequency of maneuvers depends primarily on the solar flux as it affects the Earth's atmosphere, and there are expected to be one maneuver (or series of maneuvers) every 40 to 200 days.

Each orbit maintenance maneuver is performed as two thrusts on pass 254 cycle N and 1 cycle N+1 (see plot below). Orbit computation is optimised to minimize the orbit error during such periods. Science data are taken during orbit maintenance maneuvers and will be distributed (an orbit state flag is provided in the products).

2.4.3.1.1. Equator Crossing Longitudes (in order of Pass Number)

Pass	Longitude	Pass	Longitude	Pass	Longitude	Pass	Longitude	Pass	Longitude	Pass	Longitude
1	99.9249	44	30.4744	87	321.0274	130	251.5783	173	182.1282	216	112.6813
2	265.7517	45	196.3012	88	126.8541	131	57.4042	174	347.9550	217	278.5075
3	71.5776	46	2.1280	89	292.6810	132	223.2310	175	153.7829	218	84.3343
4	237.4044	47	167.9557	90	98.5078	133	29.0576	176	319.6096	219	250.1600
5	43.2305	48	333.7825	91	264.3336	134	194.8843	177	125.4369	220	55.9867
6	209.0573	49	139.6102	92	70.1603	135	0.7117	178	291.2636	221	221.8129
7	14.8844	50	305.4370	93	235.9862	136	166.5385	179	97.0902	222	27.6397
8	180.7112	51	111.2637	94	41.8130	137	332.3659	180	262.9170	223	193.4666
9	346.5387	52	277.0905	95	207.6395	138	138.1927	181	68.7430	224	359.2934
10	152.3655	53	82.9167	96	13.4663	139	304.0198	182	234.5697	225	165.1212
11	318.1928	54	248.7435	97	179.2937	140	109.8466	183	40.3959	226	330.9479
12	124.0196	55	54.5694	98	345.1205	141	275.6727	184	206.2227	227	136.7755
13	289.8463	56	220.3962	99	150.9484	142	81.4995	185	12.0499	228	302.6023
14	95.6731	57	26.2229	100	316.7751	143	247.3252	186	177.8767	229	108.4290
15	261.4989	58	192.0497	101	122.6022	144	53.1520	187	343.7042	230	274.2558
16	67.3256	59	357.8771	102	288.4290	145	218.9782	188	149.5309	231	80.0819
17	233.1515	60	163.7039	103	94.2556	146	24.8050	189	315.3582	232	245.9087
18	38.9783	61	329.5313	104	260.0823	147	190.6320	190	121.1850	233	51.7347
19	204.8049	62	135.3580	105	65.9083	148	356.4588	191	287.0117	234	217.5614
20	10.6317	63	301.1851	106	231.7351	149	162.2866	192	92.8384	235	23.3883
21	176.4592	64	107.0119	107	37.5614	150	328.1133	193	258.6642	236	189.2150
22	342.2860	65	272.8379	108	203.3881	151	133.9409	194	64.4909	237	355.0425
23	148.1139	66	78.6647	109	9.2154	152	299.7676	195	230.3169	238	160.8693
24	313.9406	67	244.4904	110	175.0422	153	105.5943	196	36.1437	239	326.6966
25	119.7676	68	50.3172	111	340.8697	154	271.4211	197	201.9704	240	132.5234
26	285.5944	69	216.1435	112	146.6964	155	77.2471	198	7.7971	241	298.3504
27	91.4209	70	21.9702	113	312.5237	156	243.0739	199	173.6248	242	104.1772
28	257.2477	71	187.7974	114	118.3505	157	48.8999	200	339.4515	243	270.0031
29	63.0736	72	353.6242	115	284.1770	158	214.7267	201	145.2793	244	75.8299
30	228.9004	73	159.4520	116	90.0038	159	20.5536	202	311.1061	245	241.6556
31	34.7268	74	325.2788	117	255.8295	160	186.3804	203	116.9330	246	47.4824
32	200.5535	75	131.1062	118	61.6562	161	352.2079	204	282.7598	247	213.3088
33	6.3809	76	296.9330	119	227.4823	162	158.0346	205	88.5862	248	19.1355
34	172.2076	77	102.7596	120	33.3090	163	323.8620	206	254.4130	249	184.9628
35	338.0351	78	268.5864	121	199.1358	164	129.6887	207	60.2389	250	350.7896
36	143.8619	79	74.4124	122	4.9626	165	295.5157	208	226.0657	251	156.6174
37	309.6891	80	240.2392	123	170.7903	166	101.3425	209	31.8922	252	322.4442
38	115.5159	81	46.0652	124	336.6170	167	267.1683	210	197.7189	253	128.2715
39	281.3423	82	211.8920	125	142.4448	168	72.9951	211	3.5463	254	294.0983
40	87.1690	83	17.7190	126	308.2716	169	238.8209	212	169.3731		
41	252.9947	84	183.5458	127	114.0984	170	44.6477	213	335.2005		
42	58.8215	85	349.3733	128	279.9252	171	210.4741	214	141.0273		
43	224.6476	86	155.2000	129	85.7515	172	16.3009	215	306.8545		

Table 6 : Equator Crossing Longitudes (in order of Pass Number)

2.4.3.1.2. Equator Crossing Longitudes (in order of Longitude)

Pass	Longitude	Pass	Longitude	Pass	Longitude	Pass	Longitude	Pass	Longitude	Pass	Longitude
135	0.7117	118	61.6562	101	122.6022	84	183.5458	67	244.4904	50	305.4370
46	2.1280	29	63.0736	12	124.0196	249	184.9628	232	245.9087	215	306.8545
211	3.5463	194	64.4909	177	125.4369	160	186.3804	143	247.3252	126	308.2716
122	4.9626	105	65.9083	88	126.8541	71	187.7974	54	248.7435	37	309.6891
33	6.3809	16	67.3256	253	128.2715	236	189.2150	219	250.1600	202	311.1061
198	7.7971	181	68.7430	164	129.6887	147	190.6320	130	251.5783	113	312.5237
109	9.2154	92	70.1603	75	131.1062	58	192.0497	41	252.9947	24	313.9406
20	10.6317	3	71.5776	240	132.5234	223	193.4666	206	254.4130	189	315.3582
185	12.0499	168	72.9951	151	133.9409	134	194.8843	117	255.8295	100	316.7751
96	13.4663	79	74.4124	62	135.3580	45	196.3012	28	257.2477	11	318.1928
7	14.8844	244	75.8299	227	136.7755	210	197.7189	193	258.6642	176	319.6096
172	16.3009	155	77.2471	138	138.1927	121	199.1358	104	260.0823	87	321.0274
83	17.7190	66	78.6647	49	139.6102	32	200.5535	15	261.4989	252	322.4442
248	19.1355	231	80.0819	214	141.0273	197	201.9704	180	262.9170	163	323.8620
159	20.5536	142	81.4995	125	142.4448	108	203.3881	91	264.3336	74	325.2788
70	21.9702	53	82.9167	36	143.8619	19	204.8049	2	265.7517	239	326.6966
235	23.3883	218	84.3343	201	145.2793	184	206.2227	167	267.1683	150	328.1133
146	24.8050	129	85.7515	112	146.6964	95	207.6395	78	268.5864	61	329.5313
57	26.2229	40	87.1690	23	148.1139	6	209.0573	243	270.0031	226	330.9479
222	27.6397	205	88.5862	188	149.5309	171	210.4741	154	271.4211	137	332.3659
133	29.0576	116	90.0038	99	150.9484	82	211.8920	65	272.8379	48	333.7825
44	30.4744	27	91.4209	10	152.3655	247	213.3088	230	274.2558	213	335.2005
209	31.8922	192	92.8384	175	153.7829	158	214.7267	141	275.6727	124	336.6170
120	33.3090	103	94.2556	86	155.2000	69	216.1435	52	277.0905	35	338.0351
31	34.7268	14	95.6731	251	156.6174	234	217.5614	217	278.5075	200	339.4515
196	36.1437	179	97.0902	162	158.0346	145	218.9782	128	279.9252	111	340.8697
107	37.5614	90	98.5078	73	159.4520	56	220.3962	39	281.3423	22	342.2860
18	38.9783	1	99.9249	238	160.8693	221	221.8129	204	282.7598	187	343.7042
183	40.3959	166	101.3425	149	162.2866	132	223.2310	115	284.1770	98	345.1205
94	41.8130	77	102.7596	60	163.7039	43	224.6476	26	285.5944	9	346.5387
5	43.2305	242	104.1772	225	165.1212	208	226.0657	191	287.0117	174	347.9550
170	44.6477	153	105.5943	136	166.5385	119	227.4823	102	288.4290	85	349.3733
81	46.0652	64	107.0119	47	167.9557	30	228.9004	13	289.8463	250	350.7896
246	47.4824	229	108.4290	212	169.3731	195	230.3196	178	291.2636	161	352.2079
157	48.9999	140	109.8466	123	170.7903	106	231.7351	89	292.6810	72	353.6242
68	50.3172	51	111.2637	34	172.2076	17	233.1515	254	294.0983	237	355.0425
233	51.7347	216	112.6813	199	173.6248	182	234.5697	165	295.5157	148	356.4588
144	53.1520	127	114.0984	110	175.0422	93	235.9862	76	296.9330	59	357.8771
55	54.5694	38	115.5159	21	176.4592	4	237.4044	241	298.3504	224	359.2934
220	55.9867	203	116.9330	186	177.8767	169	238.8209	152	299.7676		
131	57.4042	114	118.3505	97	179.2937	80	240.2392	63	301.1851		
42	58.8215	25	119.7676	8	180.7112	245	241.6556	228	302.6023		
207	60.2389	190	121.1850	173	182.1282	156	243.0739	139	304.0198		

Table 7 : Equator Crossing Longitudes (in order of Longitude)

2.4.3.1. Geodetic Orbit (From May 2012 until End Of Life)

Below are the characteristics of the geodetic orbit which was maintained, as before, within +/- 1km control box at the Equator.

The mean classical orbit elements are given in the table below.

Orbit element	Value
Semi-major axis	7,702.437 km
Eccentricity	1.3 to 2.8 E-4
Inclination	66.042 deg

Table 8 : Mean classical orbit elements

The orbit auxiliary data are given in the table below.

Auxiliary Data	Values
Reference (Equatorial) altitude	1,324 km
Nodal period	6,730 sec (1h52'10'')
Repeat period	406 days (sub-cycles 3.9, 10.9, 47.5, 179.5 days)
Number of revolutions within a cycle	140 revolutions in a sub-cycle of 10.9 days

Table 9 : Orbit auxiliary data

2.4.4. The Jason-1 Project Phases

The satellite mission has two phases:

- The first phase, the calibration/validation phase, began when the satellite reached the operational orbit and the satellite and sensor systems were functioning normally. This phase continued until the data received from the sensors were satisfactorily calibrated and verified. The phase began shortly after launch. A preliminary calibration/validation workshop was held June 2002. A second calibration/validation workshop was held October 2002, where Jason-1 to TOPEX/POSEIDON cross validation was extensively discussed: recommendations were issued both on TOPEX/POSEIDON and Jason-1 science processing algorithms.
- The second phase, the operational phase, began April 2003 when all necessary algorithm and processing changes were implemented to have Jason-1 performances at the same level as TOPEX/POSEIDON.

2.5. Data Processing and Distribution

Processing centers, called respectively CNES SSALTO and NASA JPL POCC, include functions such as science data processing, data verification and precision orbit determination.

Processed data are placed in National archives for further distribution to the scientific community. There are three levels of processed data:

1. Telemetry data (raw data),
2. Sensor Data Records (engineering units),
3. Geophysical Data Records (geophysical units).

Geophysical data records are sent as they become available to AVISO and PO.DAAC for processing, archiving, managing, and distribution to PIs and the wider scientific community.

The operational sensor data record (OSDR), which was a non-validated product that used orbits computed by the on-board DORIS Navigator (DIODE) and did not perform ground retracking of the altimeter waveforms, were available with a latency of 3-5 hours. The interim geophysical data record (IGDR), which was also a non-validated product but that used a preliminary orbit and applied ground retracking, were available by pass with a latency of 2-3 days. The geophysical data record (GDR), which is a fully validated product that uses a precise orbit and applies ground retracking, were available operationally by repeat cycle with a latency of 30 days.

2.5.1. Access to NRT data

As the Jason-1 mission is no longer operational, the OSDRs are not available in version “e”. This section has been removed.

2.5.2. Access to off-line data

As the Jason-1 mission is no longer operational, only the GDR is available as version “e” products. These GDRs are available on PODAAC and AVISO ftp servers. Both of these archival facilities also provide a variety of auxiliary files used to produce the O/I/GDR dataset.

Data dissemination services from NASA and CNES agencies are described below.

Jason-1 data continue to be available in the original Jason-1 format, and are now also available in the same NetCDF format as the Jason-2 products. Jason-1 products are available in both formats for versions “a”, “b”, and “c” on the AVISO and PODAAC ftp servers. Jason-1 GDR version “e” products are only available in NetCDF format on the AVISO and PODAAC ftp servers.

2.5.3. Documentation

This Jason-1 User’s Handbook document describes only the native product. A description of the O/I/GDR product format and contents is provided in the CNES document “Jason-1 User Products”. All documents are available through the data dissemination services.

2.6. CNES data distribution

Users have access to Jason-1 public data through a dedicated AVISO+ ftp server with an anonymous account. Offline IGDR and GDR products are available on the following server:

IP address: avisoftp.cnes.fr

User account: anonymous

Home directory : /AVISO/pub/jason-1

With the following ftp server directory tree:

documentation	→	product handbook, reading tools, …
gdr_e	→	directory containing GDR version ‘e’ native products (with a sub directory for each cycle)
sgdr_e	→	directory containing S-GDR version ‘e’ sensor products (with a sub directory for each cycle)
ssha_gdr_e	→	directory containing GDR version ‘e’ reduced products (with a sub directory for each cycle)

Jason-1 products in their original binary format and in version “a”, “b” or “c” can be retrieved through AVISO CNES Data Center at the following address: https://aviso-data-center.cnes.fr/.

For any questions on Jason-1 data dissemination on AVISO+ servers please contact:

aviso@altimetry.fr

2.7. NASA data distribution

Users have access to Jason-1 public data through a dedicated PODAAC ftp server with an anonymous account.

The PODAAC ftp server for Jason-1 products is:

podaac.jpl.nasa.gov

Login anonymous

Jason-1 GDR-E products in NetCDF format are available on the following directories:

/allData/jason1/L2/gdr_netcdf_e → directory containing GDR native products (with a sub directory for each cycle)

/allData/jason1/L2/gdr_ssha_netcdf_e → directory containing GDR reduced products (with a sub directory for each cycle)

/allData/jason1/L2/sgdr_netcdf_e → directory containing SGDR products (with a sub directory for each cycle)

Please note that from cycle 500, Jason-1 GDR-E products (on its geodetic orbit) are available on the following directories:

/allData/jason1/L2/gdr_netcdf_e_geodetic → directory containing GDR native products (with a sub directory for each cycle)

/allData/jason1/L2/gdr_ssha_netcdf_e_geodetic → directory containing GDR reduced products (with a sub directory for each cycle)

/allData/jason1/L2/sgdr_netcdf_e_geodetic → directory containing SGDR products (with a sub directory for each cycle)

For any questions on Jason-1 data dissemination on PODAAC servers please contact:

podaac@podaac.jpl.nasa.gov.

3. Product evolution history

3.1. Models and Standards History

3.1.1. GDR Products Version "a", "b" and "c"

Please refer to previous versions of "Jason-1 products handbook" for more details about old versions of Jason-1 products.

3.1.2. GDR Products Version "e"

Note: The Jason-1 mission has not been reprocessed in version "d".

3.1.2.1. Models and Standards

The current product version is altimetric standard version "e".

The table below summarizes the models and standards that are adopted in this version of the Jason-1 GDRs. Section 3.1 provides more details on some of these models.

Model	Product Version "e"
Orbit	- DORIS and GPS tracking data for GDRs (laser ranging used for validation only)
Altimeter Retracking	<u>"Ocean MLE4" retracking</u> MLE4 fit from 2nd order Brown analytical model : MLE4 simultaneously retrieves the 4 parameters that can be inverted from the altimeter waveforms: - Epoch (tracker range offset) ⇒ altimeter range - Composite Sigma ⇒ SWH - Amplitude ⇒ Sigma0 - Square of mispointing angle <u>"Ice-1" retracking</u> Geometrical analysis of the altimeter waveforms, which retrieves the following parameters: - Epoch (tracker range offset) ⇒ altimeter range - Amplitude ⇒ Sigma0
Altimeter Instrument Corrections	One set consistent with MLE4 retracking. Improved internal path delay correction (Repeat Orbit: +60.7 and -3.2 mm in Ku- and C-band, Geodetic Orbit: +63.9 and +0.0 mm in Ku- and C-band compared to version "c", see below)
Jason-1 Microwave Radiometer (JMR) Parameters	Using JMR calibration performed at NASA/JPL in 2014 and 2015
Dry Troposphere Range Correction	From ECMWF (MARS 3D and ERA-Interim) atmospheric pressures and model for S1 and S2 atmospheric tides
Wet Troposphere Range Correction from Model	From ECMWF model (MARS 3D and ERA-Interim)
Ionosphere correction	- Based on Global Ionosphere TEC Maps from JPL - Computed from updated range and SSB.
Sea State Bias	SSB tables (Ku and C band) derived from Jason-1 altimeter data with version "e" geophysical models and orbit
Mean Sea Surface	MSS_CNES-CLS11
Mean Dynamic Topography	MDT_CNES-CLS13
Geoid	EGM2008
Bathymetry Model	DTM2000.1
Added ECMWF Re-Analysis (ERA) meteorological model	The ERA model provides alternative values for the model dry troposphere delay, model wet troposphere delay, inverse barometer correction, high frequency response to the atmosphere, and model wind speeds. The ERA alternatives are indicated with "_era" in the parameter names. The corresponding values without "_era" in the parameter names are from the operational ECMWF product.
Inverse Barometer Correction	Computed from ECMWF atmospheric (MARS 3D and ERA-Interim) pressure after removing S1 and S2 atmospheric tides
Non-tidal High-frequency Dealiasing Correction	Mog2D High Resolution ocean model on GDRs. Barotropic ocean model forced by ECMWF (MARS 3D and ERA-interim) winds and pressures; S1 and S2 atmospheric tides have been removed from the pressure field.
Tide Solution 1	GOT4.10c
Tide Solution 2	FES2014 + using GOT4.8ac load tides
Equilibrium long-period ocean tide model	from *Cartwright and Taylor* [1971] and *Cartwright and Edden* [1973] tidal potential

Model	Product Version “e”
Non-equilibrium long-period ocean tide model	Mm, Mf, Mtm, Msqm, Sa, Ssa from FES2014
Load Tide solution 1	GOT4.10c load tide (includes a tidal geocenter correction compared to GOT4.10; Desai & Ray 2014; Ray 2013)
Load Tide solution 2	GOT4.8ac load tide (includes a tidal geocenter correction compared to GOT4.8; *Desai & Ray* 2014; *Ray* 2013)
Solid Earth Tide Model	From *Cartwright and Taylor* [1971] tidal potential
Pole Tide Model	Equilibrium model using mean pole of X + iY = 0.042 + i0.293 arcseconds.
Wind Speed from Model	ECMWF model (MARS 3D and ERA-interim)
Altimeter Wind Speed Model	Derived from Jason-1 data
Rain Flag	Derived from comparisons to thresholds of the radiometer-derived integrated liquid water content and of the difference between the measured and the expected Ku-band backscatter coefficient
Ice Flag	Derived from comparison of the model wet tropospheric correction to a dual-frequency wet tropospheric correction retrieved from radiometer brightness temperatures, with a default value issued from a climatology table

Table 10 : Version “e” models and standards

3.1.2.2. Sea Surface Height Bias

In the GDR-E product version, corrections of +60.7 and -3.2 mm have been added to Ku- and C-band repeat orbit altimeter ranges reported in the version “c” products (e.g., version “e” Ku-band ranges are longer than those from version “c” by 60.7 mm) to take into account the correct internal path delay value. Similarly, corrections of +63.9 and 0.0 mm have been added to Ku- and C-band geodetic orbit altimeter ranges reported in the version “c” products. See section 5.2 for more details about altimetric ranges.

3.1.2.3. Time-tag Bias

A long period crossover point residual analysis on version “c” products showed a datation bias of about 400µs, leading to a sea surface height anomaly (SSHA) error varying with latitudes. The origin of the error has been precisely determined and its value is determined by the following formula:

$$\text{Time tag bias} = \mathrm{RA} \times \mathrm{PRI} - 2 \times \mathrm{alt}/\mathrm{c}$$

Where :

- Time tag bias = datation bias
- RA = ambiguity order (=18)
- PRI = Pulse Repetition Frequency (=1/2058.513239 or 1/ 2083.87600938 on geodetic orbit)
- alt = satellite altitude
- c = celerity

This datation bias is corrected in the Jason-1 GDR-E product version. As a result, measurement time tags on GDR-E products are slightly different to those from version “c”.

3.1.3. Orbit models

Jason-1 orbit standards for the version “e” GDRs are based on version “e” precise orbit determination (POD) standards. Its main features are summarized below. Note that version “c” GDRs used version “c” and “d” POD standards as shown in the Table below. Version “c” POD standards were applied to cycles X-Y of the version “c” GDRs, while version “d” POD standards were applied to cycles A-B of the version “c” GDRs.

	GDR-C	GDR-D

	GDR-C	GDR-D
Gravity model	EIGEN-GL04S-ANNUAL (2008) Non-tidal TVG : drifts in degree 2,3,4 zonal coeffs, C21/S21; Annual and semi-annual terms up to deg/ord 50 Solid Earth Tides: from IERS2003 conventions Ocean tides FES2004 Atmospheric gravity : 6hr NCEP pressure fields + tides from Horwitz-Cowley model Pole Tide: solid Earth and ocean from IERS2003 conventions Third bodies: Sun, Moon, Venus, Mars and Jupiter	**EIGEN-GRGS_RL02bis_MEAN-FIELD (2011)** Non-tidal TVG : Annual, Semi-annual, and **drifts up to deg/ord 50** Solid Earth Tides: from IERS2003 conventions Ocean tides FES2004 Atmospheric gravity : 6hr NCEP pressure fields + **tides from Biancale-Bode model** Pole Tide: solid Earth and ocean from IERS2010 conventions Third bodies: Sun, Moon, Venus, Mars and Jupiter
Surface forces	Radiation Pressure model: thermo-optical coefficient from pre-launch box and wing model, with smoothed Earth shadow model Earth Radiation : Knocke-Ries albedo and IR satellite model Atmospheric density model : DTM-94 for Jason, and MSIS-86 for Envisat	Unchanged
Estimated dynamical parameters	Drag coefficient every 2 or 3 revolutions Along-track and Cross-track 1/rev per day or every 12 hours	Unchanged
Satellite reference	Mass and Center of gravity: Post-Launch values + variations generated by Control Center Attitude Model : For Jason-1 and Jason-2 : Quaternions and Solar Panel orientation from control center, completed by nominal yaw steering law when necessary For Envisat: nominal attitude law	Unchanged
Displacement of reference points	Earth tides: IERS2003 conventions Ocean Loading: FES2004 Pole tide : solid earth pole tides (Pole tide and ocean loading applied to both SLR stations and DORIS beacons) Reference GPS constellation: JPL solution at IGS (orbits and clocks) , consistent with IGS05; before GPS week 1400, JPL solution has been aligned with IGS05; IGS00 clocks are unchanged	Earth tides: IERS2003 conventions Ocean Loading: FES2004 Pole tide : solid earth pole tides (Pole tide and ocean loading applied to both SLR stations and DORIS beacons) Reference GPS constellation: JPL solution at IGS (orbits and clocks) - **fully consistent with IGS08**
Terrestrial Reference	Extended ITRF2005 (SLRF/LPOD2005, DPOD2005, IGS05)	**Extended ITRF2008 (SLRF/ITRF2008, DPOD2008, IGS08)**

	GDR-C	GDR-D
Frame		
Earth orientation	Consistent with IERS2003 conventions and ITRF2005	**Consistent with IERS2010 conventions and ITRF2008**
Propagations delays	SLR Troposphere correction: Mendes-Pavlis SLR range correction: constant 5.0 cm range correction for Envisat, elevation dependent range correction for Jason DORIS Troposphere correction : CNET model GPS PCO/PCV (Emitter and Receiver) consistent with constellation orbits and clocks (IGS05 Antex after GPS week 1400) GPS : Phase wind-up correction	SLR Troposphere correction: Mendes-Pavlis SLR range correction: constant 5.0 cm range correction for Envisat, elevation dependent range correction for Jason **DORIS Troposphere correction : GPT/GMF model** GPS PCO/PCV (Emitter and Receiver) consistent with constellation orbits and clocks (**IGS08 Antex**) GPS : Phase wind-up correction
Estimated measurement parameters	DORIS: 1 Frequency bias per pass, 1 troposphere zenith bias per pass SLR : bias per arc solved for a few stations, bias per pass for a few stations GPS: Floating ambiguity per pass, receiver clock adjusted per epoch	Unchanged
Tracking Data corrections	Jason-1 Doris data: South Atlantic Anomaly Model (JM Lemoine et al.) applied before and after DORIS instrument change DORIS datation bias for Envisat and Jason aligned with SLR before and after instrument change	Unchanged
Doris Weight	1.5 mm/s (1.5 cm over 10 sec) For Jason-1 , Doris Weight is reduced by a factor 10 before Doris instrument change	Unchanged
SLR Weight	10 cm	**15 cm**
GPS Weight	10 cm (phase) / 10 m (code)	**2 cm (phase) / 2 m (code)**

Table 11. GDR-C/GDR-D orbit standard

	GDR-D	GDR-E
Gravity model	EIGEN-GRGS_RL02bis_MEAN-FIELD Non-tidal TVG: annual, semi-annual, and drift up to deg/ord 50 Solid Earth tides: from IERS2003 conventions Ocean tides: FES2004	**EIGEN-GRGS.RL03-v2.MEAN-FIELD** Non-tidal TVG: **one annual, one semi-annual, one bias and one drift terms for each year up to deg/ord 80; C21/S21 modeled according to IERS2010 conventions; C31/S31 estimation by arc if necessary** Unchanged Ocean tides: **FES2012**

	Atmospheric gravity: 6hr NCEP pressure fields (20x20) + tides from Biancale-Bode model Pole tide: solid Earth and ocean from IERS2010 conventions Third bodies: Sun, Moon, Venus, Mars and Jupiter	Atmospheric gravity: **6hr NCEP pressure fields (70x70)** + tides from Biancale-Bode model Unchanged Unchanged
Surface forces	Radiation pressure model: thermo-optical coefficient from pre-launch box and wing model, with smoothed Earth shadow model Earth radiation: Knocke-Ries albedo and IR satellite model Atmospheric density model: DTM-94 for Jason satellites, and MSIS-86 for other satellites	Radiation pressure model: **calibrated semi-empirical solar radiation pressure model** Unchanged Atmospheric density model: **DTM-13 for Jason satellites, HY-2A**, and MSIS-86 for other satellites
Estimated dynamical parameters	Drag coefficient every 2 or 3 revolutions Along-track and cross-track 1/rev per day or every 12 hours	**Improved stochastic solutions**
Satellite reference	Mass and center of gravity: post-launch values + variations generated by Control Center Attitude model: For Jason satellites: quaternions and solar panel orientation from control center, completed by nominal yaw steering law when necessary Other satellites: nominal attitude law	Unchanged
Displacement of reference points	Earth tides: IERS2003 conventions Ocean loading: FES2004 Pole tide: solid earth pole tides Reference GPS constellation: JPL solution at IGS (orbits and clocks) – fully consistent with IGS08	Unchanged Ocean loading: **FES2012** Pole tide: solid earth pole tides and ocean pole tides **(*Desai*, 2002)** **S1-S2 atmospheric pressure loading, implementation of *Ray & Ponte* (2003) by van Dam** Reference GPS constellation: **JPL solution in “native” format (orbits and clocks), referenced to the CoM of the solid Earth/Ocean system - fully consistent with IGS08**

Geocenter variations	None	**Tidal: ocean loading and S1-S2 atmospheric pressure loading** **Non-tidal: seasonal model from J. Ries**
Terrestrial Reference Frame	Extended ITRF2008 (SLRF/ITRF2008, DPOD2008, IGS08)	Unchanged
Earth orientation	Consistent with IERS2010 conventions and ITRF2008	Unchanged
Propagations delays	SLR troposphere correction: Mendes-Pavlis SLR range correction: constant 5.0 cm range correction for Envisat, elevation dependent range correction for Jason DORIS troposphere correction: GPT/GMF model GPS PCO/PCV (emitter and receiver) consistent with constellation orbits and clocks (IGS08 ANTEX) GPS: phase wind-up correction	Unchanged Unchanged Unchanged **DORIS beacons phase center correction** Unchanged Unchanged
Estimated measurement parameters	DORIS: one frequency bias per pass, one troposphere zenith bias per pass SLR: bias per arc solved for a few stations, bias per pass for a few stations GPS: floating ambiguity per pass, receiver clock adjusted per epoch	Unchanged **Reference used to evaluate orbit precision and stability** Unchanged
Tracking Data corrections	Jason-1 Doris data: South Atlantic Anomaly model (J.-M. Lemoine et al.) applied before and after DORIS instrument change DORIS time-tagging bias for Envisat and Jason aligned with SLR before and after instrument change	Jason-1 Doris data: **updated South Atlantic Anomaly model (J.-M. Lemoine et al.) applied before and after DORIS instrument change** Unchanged
Doris Weight	1.5 mm/s (1.5 cm over 10 sec)	**For Jason-1, SAA DORIS beacons weight is divided by 10 before DORIS instrument change**
SLR Weight	15 cm	**Reference used to evaluate orbit precision and stability**
GPS Weight	2 cm (phase) / 2 m (code)	Unchanged

Table 12. GDR-D/GDR-E orbit standard

3.1.4. Mean Sea Surface

The MSS_CNES-CLS11 model is computed from 16 years of satellite altimetry data from a variety of missions. Its main characteristics are the following:

Name	MSS_CNES-CLS11
Reference ellipsoid	T/P
Referencing time period	1993-2012 (~20 years)
Data covering period	1993-late 2008 (16 years)
Spatial coverage	Global (80°S to 84°N) - Oceanwide where altimetric data are available. EIGEN_GRACE_5C geoid elsewhere and on continents.
Spatial resolution	Regular grid with a 1/30° (2 minutes) spacing (i.e. ~4 km)
Grid	10801 points in longitude / 4921 points in latitude
MSS determination technique	Local least square collocation method on a 6' grid where altimetric data in a 200-km radius are selected. Estimation on a 2' grid based on SSH-geoid values (remove/restore technique to recover the full signal). The inverse method uses local anisotropic covariance functions that witness the MSS wavelength content.
Estimation error level	The Optimal Interpolation method provides a calibrated formal error. Calibrated error of the Mean Sea Surface is provided in the products.
Altimetric dataset	T/P 10 years mean profile (first orbit), T/P tandem 3 years profile ERS-2 8 years mean profile, 1 year ERS-1 (geodetic phase) GFO, 7 years mean profile Jason-1, 7 years mean profile Envisat, 7 years mean profile

Table 13 : MSS_CNES-CLS11 model characteristics

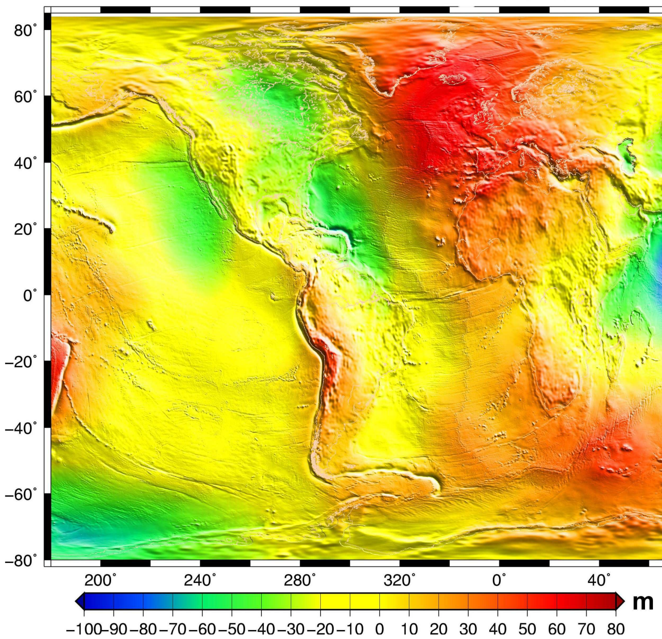

Figure 4 : Mean Sea Surface MSS_CNES-CLS11

Refer to http://www.aviso.altimetry.fr/en/data/products/auxiliary-products/mss/index.html for more details on this model.

3.1.5. Mean Dynamic Topography

The MDT_CNES-CLS013 model is computed from satellite altimetry data from a variety of missions. Its main characteristics are the following:

Name	MDT_CNES-CLS13
Referencing time period	1993-2012 (~20 years)
Domain	Global (78.25°S to 81.25°N)
Spatial resolution	Regular grid with a 1/4° (15 minutes) spacing (i.e. ~30 km)
Grid	720 points in longitudes / 320 points in latitude
MDT determination technique	Reference the altimeter Sea Level Anomalies (SLA), computed relative to a 20 year (1993-2012) mean profile, in order to obtain absolute measurements of the ocean dynamic topography. Based on : - 2 years of GOCE data, - 7 years of GRACE data, - 20 years of altimetry and in-situ data (hydrologic and drifters data).
Estimation error level	Error of the Mean Dynamic Topography is provided in the products.

Table 14 : MDT_CNES-CLS13 model characteristics

This sea surface height (mean sea surface height above geoid) corresponds to mean geostrophic currents and its changes.

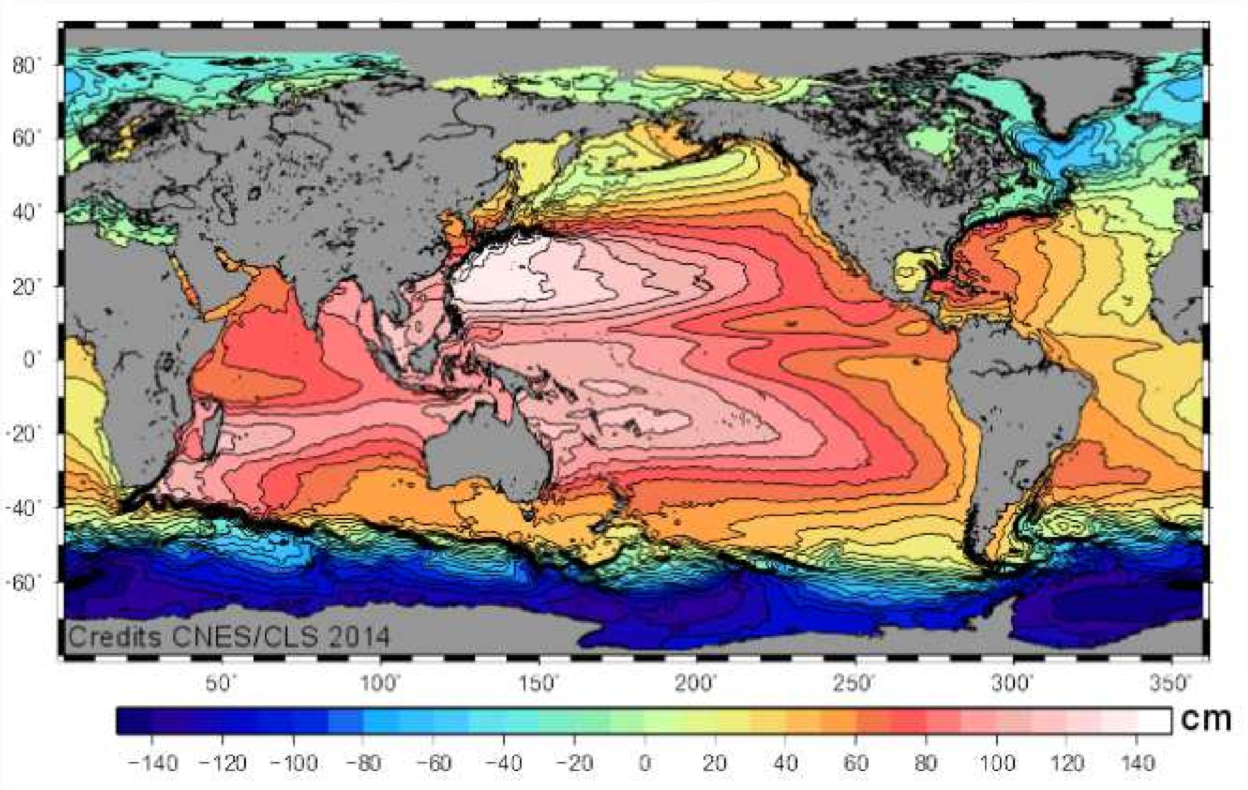

Figure 5 : Mean Dynamic Topography MDT_CNES-CLS13

Refer to http://www.aviso.altimetry.fr/en/data/products/auxiliary-products/mdt-copy-1/mdt-description.html for more details on this model.

3.1.6. Geoid

Jason-1 GDRs (version “e”) use the EGM2008 geopotential to compute the geoid.

The official Earth Gravitational Model EGM2008 has been publicly released by the U.S. National Geospatial-Intelligence Agency (NGA) EGM Development Team. This gravitational model is complete to spherical harmonic degree and order 2159, and contains additional coefficients extending to degree 2190 and order 2159.

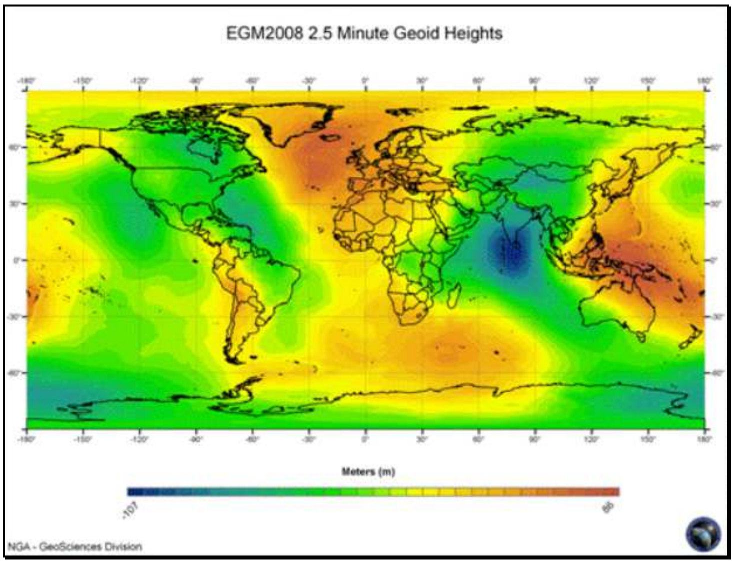

Figure 6 : EGM2008 geoid

More information on EGM96 can be found at http://earth-info.nga.mil/GandG/wgs84/gravitymod/egm2008/index.html

3.1.7. Bathymetry

The value of this parameter is determined from the DTM2000.1 model from N. Pavlis and J. Saleh [personal communication, 2000] of the Raytheon ITSS/Goddard Space Flight Center. The model is provided globally with a 2' resolution. The heritage of DTM2000.1 goes back to the OSUJAN98 database [*Pavlis and Rapp*, 1990] and the JGP95E database [Chapter 2 of *Lemoine et al.*, 1998]. The bathymetric information in DTM2000.1 (originating from *Smith and Sandwell's* [1994] global sea floor topography) has significant differences with the ETOPO5 bathymetric model. The mean and standard deviation of these differences is 10 m and 270 m, respectively.

3.1.8. Ocean Tides

The two geocentric tide values provided on the Jason-1 GDR, ocean_tide_sol1 and ocean_tide_sol2, are computed with diurnal and semidiurnal ocean and load tide values predicted by the GOT4.10c (*Ray*, 2013) and FES2014 (*Carrere et al.*, 2015) models, respectively.

Both geocentric ocean tide fields (ocean_tide_sol1 and ocean_tide_sol2) also include the load tides from the respective models (load_tide_sol1 and load_tide_sol2), and the equilibrium long-period ocean tide (ocean_tide_equil).

By essence, both models include the S1 and S2 oceanic response to atmospheric pressure.

The GOT4.10c model includes the M4 ocean tide. The FES2014 model includes 9 non-linear waves : M4, M6, M8, MN4, MS4, MKS2, N4, S4, MSf.

Note that the load tide fields (load_tide_sol1 and load_tide_sol2) include the load tides corresponding to GOT4.10c and FES2014 models respectively; the FES2014 loading tide is based on the GOT4.8ac loading tide. The GOT4.8a**c** and the GOT4.10**c** loading tide both include the tidal geocenter correction (Desai and Ray. 2014).

Moreover note that both models ocean tidal atlas have been extrapolated along the shores in order to avoid any altimeter missing measurement due to an undefined tidal solution: GOT4.10c model was extrapolated on 1 pixel of 0.5°, and FES2014 on 10 pixels of 1/16°.Both models are interpolated to provide the geocentric ocean and load tides at the location of the altimeter measurement, and an interpolation quality flag is provided on the GDRs to indicate the quality of this interpolation (see interp_flag_ocean_tide_sol1 and interp_flag_ocean_tide_sol2).

The ocean_tide_non_equil field contains the difference between the dynamic (non-equilibrium) long-period ocean tide computed from FES2014 model and the equilibrium long-period ocean tide field (ocean_tide_equil): this parameter is computed as a correction to the parameter ocean_tide_equil.

3.1.8.1. GOT4.10c

The GOT4.10c model is a recent version of the GOT models developed by R. Ray (Ray, 2013).

The solution consists of independent near-global estimates of 10 constituents (K1, K2, M2, M4, N2,O1, P1, Q1, S1, S2). An a priori model was used that consisted of the hydrodynamic model FES 2004 [Lyard et al. 2006], and several other local hydrodynamic models.

GOT4.10c is identical to 4.7, 4.8, and 4.9, except that only data from Jason-1 and Jason-2 were used, with no T/P data. Otherwise, all other processing and data were kept unchanged. Note that the dry-tropospheric correction for the Jason satellites never had the S2 air-tide error that the original T/P data had. The “c” in the model name indicates that the model includes the tidal geocenter correction (Desai and Ray, 2014).

3.1.8.2. FES2014

FES2014 is the most recent version of the FES (Finite Element Solution) tide model developed in 2014-2015 (*Carrrere et al.*, 2015). It is an improved version of FES2012, which was a fully revised version of the global hydrodynamic tide solutions initiated by the works of Christian (*Le Provost et al.*, 1995) in the early nineties. The new model has been developed, implemented and validated by LEGOS, NOVELTIS and CLS teams, within a CNES funded project.

FES2014 takes advantage of longer altimeter time series and better altimetry standards, improved modeling and data assimilation techniques, and more accurate ocean bathymetry. Special efforts have been dedicated to address the major non-linear tides issue and to the determination of accurate tidal currents.

FES2014 is based on the resolution of the tidal barotropic equations (T-UGO model) in a spectral configuration. A new original high resolution global bathymetry was built including several regional databases, and a new global finite element grid (~3 millions of nodes) is used leading to a twice more accurate 'free' solution (independent of in situ and remote-sensing data) than the FES2012 version.

Then the accuracy of this 'free' solution was improved by assimilating long-term altimetry data (Topex-Poseidon/Jason-1/Jason-2, TPN/J1N, ERS-1/ ERS-2/ ENVISAT) and tidal gauges, through an improved representer assimilation method.

The final FES2014 solution shows strong improvement compared to FES2012, GOT4.10 and DTU10 models, particularly in coastal and shelf regions, and also in some deep ocean regions and in large parts of the Arctic Ocean.

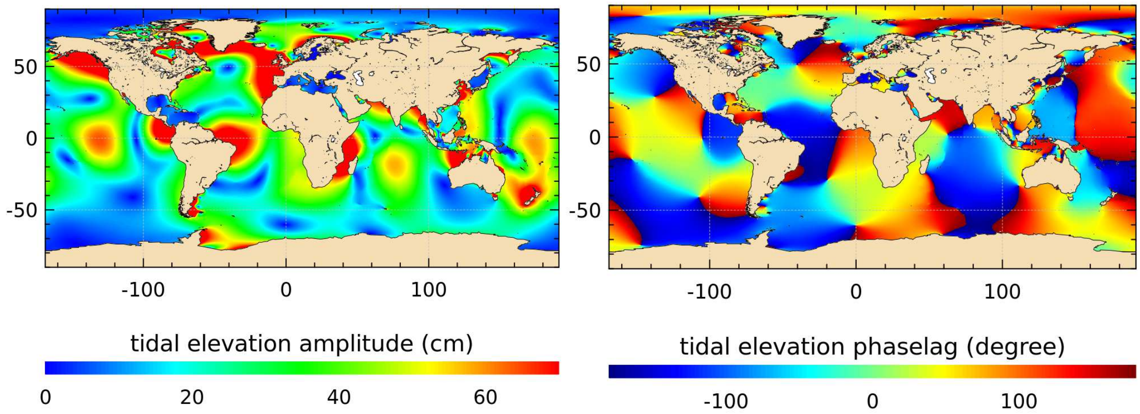

Figure 7. Amplitude and phase of the FES2014 model.

3.1.9. Data Editing Criteria

The following editing criteria are a recommended guideline for finding good records from the GDR to calculate the sea level anomaly from the Ku band range. The user should review these criteria before using them and may wish to modify them.

First, check the following conditions to retain only ocean data and remove any bad, missing, or flagged data:

Parameter	Value	Meaning
surface_type	0	Open oceans or semi-enclosed seas
ice_flag	0	No ice

Table 15 : Recommended editing criteria

Then, filter the data as follows to retain only the most valid data:

Parameter	Validity conditions
range_numval_ku	10 ≤ x
range_rms_ku	0 ≤ x (mm) ≤ 200
altitude - range_ku	-130 000 ≤ x (mm) ≤ 100 000
model_dry_tropo_corr	-2 500 ≤ x (mm) ≤ - 1 900
rad_wet_tropo_corr	-500 ≤ x (mm) ≤ - 1
iono_corr_alt_ku	-400 ≤ x (mm) ≤ 40
sea_state_bias_ku	-500 ≤ x (mm) ≤ 0
ocean_tide_sol1	-5 000 ≤ x (mm) ≤ 5 000
solid_earth_tide	-1 000 ≤ x (mm) ≤ 1 000
pole_tide	-150 ≤ x (mm) ≤ 150
swh_ku	0 ≤ x (mm) ≤ 11 000
sig0_ku	7 ≤ x (dB) ≤ 30
wind_speed_alt	-0 ≤ x (m/s) ≤ 30
sig0_rms_ku	x (dB) ≤ 1
sig0_numval_ku	10 < x
off_nadir_angle_ku_wvf	-0.2 < (deg^2) < 0.5

Table 16 : Recommended filtering criteria

To restrict studies to deep water, apply a limit, e.g., water depth of 1000m or greater, using the bathymetry parameter (ocean depth in meters.)

Please note that for GDR version “e”, a surface_type_globcover has been added to the product. It is a flag with 7 states computed from a mask built with MODIS and GlobCover data (0 = Open ocean; 1 = Land; 2 = Continental waters; 3 = Aquatic vegetation; 4 = Continental ice and snow; 5 = Floating ice; 6 = Salted basin). Users should use these more refined area definition for specific studies in non-open ocean (recommended filtering criteria above may not apply as they are recommended for ocean only).

4. Using the GDR data

4.1. Overview

This section will give the reader a guide to the use of the Jason-1 GDR data. Remember that this is research data. While this handbook tries to be correct and complete, nothing can replace the information to be gained at conferences and other meetings of those using these data. Information is also available on the PODAAC and AVISO+ web servers. The reader must proceed with caution and at his or her own risk. Please direct questions and comments to the contacts given on the last page of this handbook.

The instruments on Jason-1 make direct observations of the following quantities: altimeter range, ocean significant wave height, ocean radar backscatter cross-section (a measure of wind speed), ionospheric electron content in the nadir direction, tropospheric water content, and position relative to the GPS satellite constellation. The GPS data and ground-based DORIS measurements of the satellite location and speeds are used in the precision orbit determination (POD) of the satellite, and ground-based laser station measurements are used to validate the POD solution. All of these measurements are useful in themselves, but they are made primarily to derive the sea surface height with the highest possible accuracy. Such a computation also needs external data (not collected aboard Jason-1), e.g., atmospheric pressure, etc. In addition, instrument health and calibration data are collected onboard and used to make corrections to the main measurements and to monitor the instrument stability on the long term.

The GDR contains all relevant corrections needed to calculate the sea surface height. For the other "geophysical variables" in the product: ocean significant wave height, tropospheric water content, ionospheric electron content (derived by a simple formula), and wind speed, the needed instrument and atmospheric corrections have already been applied.

The following sections explain the rationale for how the corrections should be applied.

4.2. Typical computation from altimetry data

In this section references are made to specific GDR parameters by name using the name of the variable as described in the NetCDF data sets. For example, surface_type is a flag parameter indicating, among other things, whether or not the data point is over open ocean.

WARNING

Default values are given to data when computed values are not available (See section 6.1.2.4) so users should screen parameters to avoid using those with default values. Also users should check flag values. The related flags are given in the description of each variable (See section 6.1.2.4) although some discussion of flags appears in this section.

4.2.1. Corrected Altimeter Range

The main data of the GDR are the altimeter ranges. The GDR provides ranges measured at Ku-band (range_ku) and C-band (range_c). The Ku-band range is used for most applications. The reported ranges are corrected for instrument effects, including the instrument corrections (net_instr_corr_ku and net_instr_corr_c). Instrument corrections are separately reported for each of the Ku and C band ranges (net_instr_corr_ku and net_instr_corr_c). The reported ranges must be corrected for path delay in the atmosphere through which the radar pulse passes and the nature of the reflecting sea surface. Recall all range corrections are defined so they should be ADDED to the range. The corrected range is given by:

Corrected Range = Range	+ Wet Troposphere Correction + Dry Troposphere Correction + Ionosphere Correction

+ Sea State Bias Correction

Wet Troposphere Correction :

Use JMR correction (rad_wet_tropo_corr).

Dry Troposphere Correction :

Use model correction (model_dry_tropo_corr or model_dry_tropo_corr_era).

Ionosphere Correction :

Use altimeter ionosphere correction (iono_corr_alt_ku to correct range_ku).

IMPORTANT: See Section 4.2.4 "Smoothing the Ionosphere Correction".

Sea State Bias Correction : Use sea state bias correction (sea_state_bias_ku to correct range_ku).

NOTE: The ionosphere and sea state bias corrections are both frequency dependent. Therefore Ku band corrections should only be applied to Ku band ranges, and C band corrections should only be applied to C band ranges. Section 4.8 explains how the C band ionosphere correction can be derived from the Ku band ionosphere correction (iono_corr_alt_ku), while the C band sea state bias correction is provided as sea_state_bias_c.

4.2.2. Sea Surface Height and Sea Level Anomaly

Sea surface height (SSH) is the height of the sea surface above the reference ellipsoid. It is calculated by subtracting the corrected range from the Altitude:

Sea Surface Height = Altitude - Corrected Range

The sea level anomaly (SLA), also referred to as Residual Sea Surface, is defined here as the sea surface height minus the mean sea surface and minus known geophysical effects, e.g., tidal and inverse barometer. It is given by:

Sea Level Anomaly = Sea Surface Height	- Mean Sea Surface
	- Solid Earth Tide Height
	- Geocentric Ocean Tide Height
	- Pole Tide Height
	- Inverted Barometer Height Correction
	- HF Fluctuations of the Sea Surface Topography

The SLA contains information about:

- Real changes in ocean topography related to ocean currents
- Dynamic response to atmospheric pressure
- Differences between the tide model and observed tides
- Differences between the mean sea surface model and the true mean sea surface at the Jason-1 location
- Unmodeled or mismodeled measurement effects (skewness, sea state bias, altimeter errors, tropospheric corrections, ionospheric correction, etc.)
- Orbit errors

There is naturally also random measurement noise. Understanding the first four items as a function of space and time is the purpose of Jason-1.

Altitude : Orbit altitude (see parameter altitude)

Corrected Range : is defined above.

Tide effects (solid earth tide height, geocentric ocean tide height, pole tide height)**:** See sections 4.2.2.1 and 5.9.

Inverted Barometer Height Correction : Use inv_bar_corr or inv_bar_corr_era (see also section 5.10).

HF Fluctuations of the Sea Surface Topography : Use hf_fluctuations_corr or hf_fluctuations_corr_era (see also section 5.10).

Mean Sea Surface : See sections 4.2.2.2 and 5.4.

4.2.2.1. Tide Effects

The total tide effect on the sea surface height is the sum of three values from the GDR:

Tide Effect = Geocentric Ocean Tide + Solid Earth Tide + Pole Tide

(See also section 5.9 and subsections)

Geocentric Ocean Tide :

The geocentric ocean tide provided on the GDR is actually the sum total of the ocean tide with respect to the ocean bottom, and the loading tide height of the ocean bottom.

Geocentric Ocean Tide = Ocean Tide + Load Tide

The GDR provides a choice of two geocentric ocean tide values, ocean_tide_sol1 and ocean_tide_sol2. Each uses a different model for the sum total of the ocean tide and loading tide heights from the diurnal and semidiurnal tides, but both include an equilibrium representation of the long-period ocean tides at all periods except for the zero frequency (permanent tide) term. Note that the GDR also explicitly provides the loading tide height from each of the two models that are used to determine the two geocentric ocean tide values, load_tide_sol1, load_tide_sol2. The geocentric ocean tide values and loading tide values should not be used simultaneously, since the loading tide height would be modeled twice.

Solid Earth Tide :

Use solid_earth_tide

NOTE: Zero frequency (permanent tide) term also not included in this parameter.

Pole Tide :

Use pole_tide

The tide values all have the same sign/sense in that positive numbers indicate that the surface is farther from the center of the Earth.

4.2.2.2. Geophysical Surface - Mean Sea Surface or Geoid

The geophysical fields Geoid (geoid) - actually geoid undulation, but called simply geoid - and Mean Sea Surface (mean_sea_surface) are distances above the reference ellipsoid, as is the Sea Surface Height. These values are for the location indicated by latitude and longitude. If the values of these fields are needed at a different location within the current frame, along-track interpolation may be done using the high rate (20/second) range and altitude values.

As the geoid is derived from the mean sea surface, the latter is the better-known quantity. The residual surface with respect to the geoid is sometimes called the "dynamic topography" of the ocean surface.

See also discussions of mean sea surface and geoid in sections 5.3 and 5.4.

4.2.3. Mean Sea Surface and Adjustment of the Cross Track Gradient

In order to study sea level changes between two dates, it is necessary to difference sea surface heights from different cycles at the exact same latitude-longitude, so that the not well-known time-invariant geoid cancels out. However, the GDR samples are not given at the same latitude-longitude on different cycles. They are given approximately every 1 sec along the pass (about 6 km, the time difference and distance vary slightly with satellite height above the surface), and the satellite ground track is allowed to drift by $\pm$1 km. This introduces a problem: on different cycles the satellite will sample a different geoid profile. This effect is the so-called cross-track geoid gradient, and *Brenner et al.* [1990] estimated it at about 2 cm/km over most of the ocean, larger over continental slopes, reaching 20 cm/km at trenches. Even if the passes repeated exactly, one would have to interpolate along the pass (say, to a fixed set of latitudes) because a 3 km mismatch in along pass position would cause approximately a 6 cm difference in the geoid, which would mistakenly be interpreted as a change in oceanographic conditions.

Both problems are simultaneously solved if the quantity one interpolates along a given pass is the difference

Residual Height – Mean Sea Surface

Then the real geoid changes across the track are automatically accounted for (to the extent the MSS model is close to the true geoid) because the MSS is spatially interpolated to the actual satellite latitude-longitude in the GDR. The residual height term above is the residual sea surface height after applying all the tidal, atmospheric and ionospheric corrections, etc. Otherwise, those need to be interpolated separately.

One possible approach is to interpolate along track to a set of common points, a "reference" track. The reference could be:

- An actual pass with maximum data and/or minimum gaps, or
- A specially constructed fixed track (see below)

The procedure is the following:

- For each common point, find neighboring points in the pass of interest (POI).
- In the POI, interpolate along track to the common point, using longitude as the independent variable, for each quantity of interest - sea surface height (see above), mean sea surface, geoid, tides, etc.
- As stated above, the quantity to compare at each common point is :

  ΔSSH = Interpolated POI SSH - Interpolated POI MSS

- Other geophysical corrections must be applied to ΔSSH, depending on the type of investigation.

The geoid model in the GDR could substitute the MSS model, but its use will result in reduced accuracy in the interpolation because the resolution of the geoid undulation is lower than that of the MSS.

Desirable features of a fixed reference track include:

- Equal spacing of points (good for FFT)
- Independent variable = (point longitude - pass equator crossing longitude)
- Equator is a point (simplifies calculation)
- Point density similar to original data density

With these specifications, it is possible to make only two fixed tracks, one ascending and one descending, which will serve for all passes. The template pass is then shifted by the equator crossing longitude (global attribute of the product, see 6.2) of each pass. Recall that the equator longitude is from a predicted orbit (not updated during GDR processing). Improved accuracy can be obtained by interpolating in the latitude, longitude values. When one interpolates to the reference track, it is good practice to check that the interpolated latitude from the data records used is close to the latitude on the reference track.

4.2.4. Smoothing Ionosphere Correction

The ionospheric (range) correction is expected to be negative, but positive values are allowed up to +40 mm to accommodate instrument noise effects. To reduce the noise, it is recommended to average over 100 km or more [*Imel*, 1994], which usually results in negative numbers.

In order to provide a reversible correction, no averaging is performed on the ionospheric correction provided on the GDR. The users may smooth the ionospheric correction and apply it as follows:

- Smooth iono_corr_alt_ku as desired. Care should be taken regarding flagged data, editing criteria, and in the case of data (land) gaps. Typical/maximum smoothing scales are 100-150 km (20-25 frames) for local times between 06 and 24 hours and 150-200 km (25-35 frames) for local times between 00 and 06 hours. The shorter (longer) smoothing time is also more appropriate during times of high (low) solar activity.
- Apply the smoothed ionospheric correction to sea surface height as shown earlier.

4.2.5. Total Electron Content from Ionosphere Correction

To calculate Ionospheric Total Electron Content, TEC, use the following formula:

$$\text{Ionospheric Total Electron Content} = -\frac{dR * f^2}{40.3}$$

Where :

- Ionospheric Total Electron Content is in electrons/m^2
- dR = Ku band ionospheric range correction from the GDR in meters (iono_corr_alt_ku)
- f = frequency in Hz (13.575 GHz for the Ku band)

Note that the TEC could then be converted to a C band ionosphere range correction using the same formula above, but with the C band frequency of 5.3 GHz.

4.2.6. Range Compression

Each 1Hz frame of the Poseidon-2 Ku and C band range measurements (range_ku and range_c) are derived from the linear regression of the respective valid 20 Hz range measurements (range_20hz_ku and range_20hz_c).

An iterative outlier detection scheme is adopted in this linear regression and the resulting 20 Hz measurements are identified by setting the corresponding bit in the parameters (range_used_20hz_ku and range_used_20hz_c) to 1. Measurements not considered as outliers have the parameters (range_used_20hz_ku and range_used_20hz_c) set to 0.

The number of valid 20 Hz measurements that are used to derive each of the 1 Hz measurements is provided on the GDRs (range_numval_ku and range_numval_c,), as are the root-mean-square of the differences between the valid 20 Hz measurements and the derived 1 Hz measurement (range_rms_ku and range_rms_c).

Specialized applications, such as over land, ice, lakes or rivers, may require that the users perform their own compression algorithm on the 20 Hz measurements.

5. Altimetric data

This section presents a short discussion of the main quantities on the GDR.

An excellent overview of the theoretical and practical effects of radar altimetry is the "Satellite Altimetry" Chapter by *Chelton et al* [2001].

5.1. Precise Orbits

CNES has the responsibility for producing the orbit ephemerides for the Jason-1 data products. The Jason-1 IGDRs provided a preliminary orbit that has radial accuracies better than 4 cm (RMS), while the GDRs provide a precise orbit that has radial accuracies better than 2.5 cm (RMS). DORIS tracking data were used to compute the preliminary orbit, while DORIS and GPS tracking data are used to compute the precise orbit (laser ranging data are used for validation).

5.2. Altimeter Range

An altimeter operates by sending out a short pulse of radiation and measuring the time required for the pulse to return from the sea surface. This measurement, called the altimeter range, gives the distance between the instrument and the sea surface, provided that the velocity of the propagation of the pulse and the precise arrival time are known. The dual frequency altimeter on Jason-1 performs range measurements at the Ku and C band frequencies (see range_ku and range_c), enabling measurements of the range and the total electron content (see discussion below on ionosphere). While both range measurements are provided on the GDR (see range_ku and range_c), the Ku band range measurement has much higher accuracy than the C band measurement.

The range reported on the Jason-1 GDR has already been corrected for a variety of calibration and instrument effects, including calibration errors, pointing angle errors, center of gravity motion, and terms related to the altimeter acceleration such as Doppler shift and oscillator drift. The sum total of these corrections also appears on the GDR for each of the Ku and C band ranges (see net_instr_corr_ku and net_instr_corr_c).

A change has to be noted when Jason-1 moved on its geodetic orbit (May 2012): In order to account for the altitude change to the new geodetic orbit (May 2012), the altimeter's PRF/PRI has been updated (old value: 2059.6792 Hz / new value: 2083.87600938 Hz). Moreover, it has been decided to take the opportunity of this change to increase the accuracy of this parameter in the processing chain. This has an impact on range bias of +3.2 mm.

In the version "e" of GDR products, a datation bias has been corrected (see section 0 about time-tag bias for more details). Moreover corrections of +60.7 and -3.2 mm have been applied to the Ku- and C-band altimeter ranges, respectively, during the repeat orbit to take into account the correct internal path delay value (combination of reference plane, internal path delay and PRF/PRI truncature). During the geodetic orbit, corrections of +63.9 and 0.0 mm have been applied to the Ku- and C-band ranges as the correct value of the altimeter PRF/PRI was used in GDR-C processing.

Nominal Orbit	Ku band	C band
Reference plane	18.092	18.092
Altimeter internal path delay	-11.70211	-18.092
PRF truncature effect	-0.316	-0.316
Sum (cms)	6.07389	-0.316

Geodetic Orbit	Ku band	C band
Reference plane	18.092	18.092
Altimeter internal path delay	-11.70211	-18.092
PRF truncature effect	0	0
Sum (cms)	6.38989	0

5.3. Geoid

The geoid is an equipotential surface of the Earth's gravity field that is closely associated with the location of the mean sea surface. The reference ellipsoid is a bi-axial ellipsoid of revolution. The center of the ellipsoid is ideally at the center of mass of the Earth although the center is usually placed at the origin of the reference frame in which a satellite orbit is calculated and tracking station positions given. The separation between the geoid and the reference ellipsoid is the geoid undulation (see geoid parameter).

The geoid undulation, over the entire Earth, has a root mean square value of 30.6 m with extreme values of approximately 83 m and -106 m. Although the geoid undulations are primarily long wavelength phenomena, short wavelength changes in the geoid undulation are seen over seamounts, trenches, ridges, etc., in the oceans. The calculation of a high resolution geoid requires high resolution surface gravity data in the region of interest as well as a potential coefficient model that can be used to define the long and medium wavelengths of the Earth's gravitational field. Surface gravity data are generally only available in certain regions of the Earth and spherical harmonic expansions of the Earth's gravitational potential are usually used to define the geoid globally. Currently, such expansions are available to degree 360 and in some cases higher.

For ocean circulation studies, it is important that the long wavelength part of the geoid be accurately determined.

5.4. Mean Sea Surface

A Mean Sea Surface (MSS) represents the position of the ocean surface averaged over an appropriate time period to remove annual, semi-annual, seasonal, and spurious sea surface height signals. A MSS is given as a grid with spacing consistent with the altimeter and other data used in the generation of the grid values. The MSS grid can be useful for data editing purposes, for the calculation of along track and cross track geoid gradients, for the calculation of gridded gravity anomalies, for geophysical studies, for a reference surface to which sea surface height data from different altimeter missions can be reduced, etc. The Jason-1 GDR provides a global MSS model that is generated from multiple satellite altimetry missions.

Longer time spans of data that become available in the future, along with improved data handling techniques will improve the current MSS models. Care must be given to the retention of high frequency signal and the reduction of high frequency noise.

The Optimal Interpolation method provides a calibrated formal error which is provided in the products.

5.5. Mean Dynamic Topography

A Mean Dynamic Topography (MDT) represents the Mean Sea Surface referenced to a geoid and corrected from geophysical effects. A MDT is given as a grid with spacing consistent with the altimeter and other data used in the generation of the grid values. The MDT provides the absolute reference surface for the ocean circulation. The Jason-1 GDR provides a global MDT model that is a combined product recovering several years based on GRACE mission, altimetry and in situ data (hydrologic and drifters data).

The error on the Mean Dynamic Topography is provided in the products.

5.6. Geophysical Corrections

The atmosphere and ionosphere slow the velocity of radio pulses at a rate proportional to the total mass of the atmosphere, the mass of water vapor in the atmosphere, and the number of free electrons in the ionosphere. In addition, radio pulses do not reflect from the mean sea level but from a level that depends on wave height and wind speed. The errors due to these processes cannot be ignored and must be removed. Discussions of these effects are given in *Chelton et al.* [2001].

5.6.1. Troposphere (dry and wet)

The propagation velocity of a radio pulse is slowed by the "dry" gases and the quantity of water vapor in the Earth's troposphere. The "dry" gas contribution is nearly constant and produces height errors of approximately -2.3 m. The water vapor in the troposphere is quite variable and unpredictable and produces a height calculation error of -6 cm to -40 cm. However, these effects can be measured or modeled as discussed below.

The gases in the troposphere contribute to the index of refraction. In detail, the refractive index depends on pressure and temperature. When hydrostatic equilibrium and the ideal gas law are assumed, the vertically integrated range delay is a function only of the surface pressure, see *Chelton et al.* [2001]. The dry meteorological tropospheric range correction is principally equal to the surface pressure multiplied by -2.277mm/mbar, with a small adjustment also necessary to reflect a small latitude dependence (see model_dry_tropo_corr and model_dry_tropo_corr_era parameter).

$$\text{model\_dry\_tropo\_corr} = -2.277 * P_{atm} * [1 + 0.0026 * \cos(2 * \text{phi})]$$

where P_{atm} is surface atmospheric pressure in mbar, phi is latitude, and model_dry_tropo_corr (or model_dry_tropo_corr_era) is the dry troposphere correction in mm. There is no straightforward way of measuring the nadir surface pressure from a satellite, so it is determined from the European Center for Medium Range Weather Forecasting (ECMWF) numerical weather prediction model. The uncertainty on the ECMWF atmospheric pressure products is somewhat dependent on location. Typical errors vary from 1 mbar in the northern Atlantic Ocean to a few mbars in the southern Pacific Ocean. A 1-mbar error in pressure translates into a 2.3 mm error in the dry tropospheric correction.

The amount of water vapor present along the path length contributes to the index of refraction of the Earth's atmosphere. Its contribution to the delay of the radio pulse, the wet tropospheric delay, can be estimated by measuring the atmospheric brightness near the water vapor line at 22.2356 GHz and providing suitable removal of the background. The Jason-1 Microwave Radiometer (JMR) measures the brightness temperatures in the nadir path at 18.7, 23.8 and 34.0 GHz: the water vapor signal is sensed by the 23.8 GHz channel, while the 18.7 GHz channel removes the surface emission (wind speed influence), and the 34 GHz channel removes other atmospheric contributions (cloud cover influence) [*Keihm et al.*, 1995]. Measurements are combined to obtain the path delay in the satellite range measurement due to the water vapor content (see rad_wet_tropo_corr parameter). The uncertainty is less than 1.2 cm RMS [e.g. *Cruz Pol et al.*, 1998 and *Ruf et al.*, 1994].

Since the 2014 recalibration of JMR data, an improved near land wet path delay algorithm is applied to improve the performance up to the coast. The algorithm error when applied to the JMR is estimated to be less than 0.8 cm up to 15 km from land, less than 1.0 cm within 10 km from land, less than 1.2 cm within 5 km from land and less than 1.5 cm up to the coastline. This is estimated from detailed simulations and validated by comparisons with measured AMR data [*Brown*, 2009]. The radiometer surface type (see rad_surf_type parameter) indicates the quality of this wet tropospheric correction.

The ECMWF numerical weather prediction model also provides a value for the wet tropospheric delay. An interpolated value from this model is included in the GDR, as a backup to the measurement from the JMR (see model_wet_tropo_corr or model_wet_tropo_corr_era). This backup will prove useful when sun glint, land contamination, or anomalous sensor behavior makes the JMR measurement of the wet tropospheric delay unusable.

5.6.2. Ionosphere

At the frequencies used by the Poseidon-2 altimeter, the propagation velocity of a radio pulse is slowed by an amount proportional to the density of free electrons of the Earth's ionosphere, also known as the total electron content (TEC). The retardation of velocity is inversely proportional to frequency squared. For instance, it causes the altimeter to slightly over-estimate the range to the sea surface by typically 0.2 to 20 cm at 13.6 GHz. The amount varies from day to night (there are fewer free electrons at night), from summer to winter, and as a function of the solar cycle (there are fewer during solar minimum.) (For discussions on this correction, see *Chelton et al.* [2001], *Imel* [1994], and *Callahan* [1984]. Also, see section 4.2.4 on smoothing the ionospheric correction).

Because this effect is dispersive, measuring the range at two frequencies allows it to be estimated. Under typical ocean conditions of 2-meter significant wave height, the Ku band ionospheric range correction determined from the dual frequency measurements from the altimeter is expected to have an accuracy of ±0.5 cm (see iono_corr_alt_ku parameter).

A backup ionospheric correction solution, derived from Global Ionosphere Maps (GIM), is provided in the GDR products. It may be used over non ocean surfaces (ice, land, etc.).

5.6.3. Ocean Waves (sea state bias)

Unlike the preceding effects, sea-state effects are an intrinsic property of the large footprint radar measurements. The surface scattering elements do not contribute equally to the radar return; troughs of waves tend to reflect altimeter pulses better than do crests. Thus the centroid of the mean reflecting surface is shifted away from mean sea level towards the troughs of the waves. The shift, referred to as the electromagnetic (EM) bias, causes the altimeter to overestimate the range (see *Rodriguez et al.*, [1992]). In addition, a skewness bias also exists from the assumption in the onboard algorithms that the probability density function of heights is symmetric, while in reality it is skewed. Finally, there is a tracker bias, which is a purely instrumental effect. The sum of EM bias, skewness bias, and tracker bias is called 'sea state bias' (see sea_state_bias_ku and sea_state_bias_c parameters).

The accuracy of sea state bias models remains limited and continues to be a topic of research. The current most accurate estimates are obtained using empirical models derived from analyses of the altimeter data. The sea state bias is computed from a bilinear interpolation of a table of sea state biases versus significant wave height and wind speed, based on empirical fits (*Tran et al.*[2011]). For a typical significant wave height (SWH) of 2 meters, the sea state bias is about 10 cm, and the error (bias) in the sea state bias correction is approximately 1-2 cm. The noise of the sea state bias estimates depends mainly on the noise on the significant wave height estimates.

In the version “e” of GDR products, the Jason-1 SSB (Ku and C-band) have been recomputed at the end of 2015 based on 3-year of data from cycles 1 to 111. The products used are the GDR_E 2.0 like (GDR_E 1.3 + updates (i.e. correct bias for range + GOT4.10 using all waves)). The obtained SSB tables are then biased by +0.8 mm for the Ku-band and –28.5 mm for the C-band. These biases have been provided by S. Desai to avoid positive C-band SSB corrections. For more information please refer to:
http://meetings.aviso.altimetry.fr/fileadmin/user_upload/tx_ausyclsseminar/files/GDRE_CalVal_cnesjpl.pdf

5.7. Rain Flag

Liquid water along the pulse's path reduces the energy returned to the altimeter, mainly at Ku band. In heavy rain, there are competing effects from attenuation and surface changes. The small-scale nature of rain cells tends to produce rapid changes in the strength of the echo as the altimeter crosses rain cells. Both effects degrade the performance of the altimeter. Data contaminated by rain are rare (most are located in the west equatorial pacific), flagged and should be ignored (see rain_flag parameter).

The rain flag on the Jason-1 GDR is set if integrated liquid water content measured by the JMR is larger than a specified threshold, AND if the difference between the expected Ku-band backscatter coefficient (estimated from the C-band backscatter coefficient which is much less affected by rain) and the measured Ku-band backscatter coefficient, is larger than either a specified threshold or a specified multiple of the uncertainty in the expected Ku-band backscatter coefficient (see rain_flag parameter) [*Tournadre and Morland*, 1998] (and RD 3). Ku band backscatter coefficient used for the rain flag determination is issued from MLE4 retracking (sig0_ku and sig0_c).

A radiometer derived rain flag (see rad_rain_flag parameter) is also computed through a comparison of the 18.7 GHz brightness temperature and the cloud liquid water observed by the JMR to specific thresholds. Rain is very absorptive in the microwave, and, over ocean, increases significantly and proportional to the rain rate the brightness temperature and the cloud liquid water observed by the JMR. Over the ocean, only rain will cause the 18.7 GHz brightness temperature to rise above ~200 K.

5.8. Ice Flag

The range measurement from the altimeter is likely to have larger errors when the pulse is reflected off ice surfaces. The ice surface is not at sea level, but at some unknown distance above it. For this reason the Jason-1 GDR provides an ice flag (see ice_flag parameter) to indicate when the data point is likely to be over ice.

The ice flag is set if the absolute value of the difference between the model wet tropospheric correction and the dual frequency wet tropospheric correction retrieved from 23.8 GHz and 34.0 GHz brightness temperatures exceeds a specified threshold, OR if the number of valid 20-Hz altimeter range of the processed measurement is smaller than a specified threshold. If the corresponding computations cannot be performed, then the ice flag is set if a climatological map predicts ice at the given location, and if the wind speed derived from the altimeter measurement is less than 1 m/s, i.e., the backscatter is larger than normally expected from the ocean.

A radiometer derived sea ice flag (see rad_sea_ice_flag) is also computed through the comparison between the JMR 34.0 GHz channels and 18.7 GHz brightness temperatures. Sea ice has an emissivity near 1 in the microwave and has a small frequency dependence. This contrasts from the open ocean brightness temperature. The difference between the JMR 34.0 GHz channels and 18.7 GHz channels is near 20-30 K in the open ocean, but generally less than 10K when sea ice is present. As the difference is also small for land, sea ice presence is assessed using the radiometer surface type flag.

5.9. Tides

Tides are a significant contributor to the observed sea surface height [*Le Provost*, 2001]. While they are of interest in themselves, they have more variation than all other time-varying ocean signals. Since they are highly predictable, they are removed from the data in order to study ocean circulation. The T/P orbit was specifically selected (inclination and altitude) so that diurnal and semidiurnal tides would not be aliased to low frequencies.

There are several contributions to the tidal effect: the ocean tide, the load tide, the solid earth tide and the pole tide. The ocean tide, load tide and solid earth tide are all related to luni-solar forcing of the earth, either directly as is the case of the ocean and solid earth tide, or indirectly as is the case with the load tide since it is forced by the ocean tide. The pole tide is due to variations in the earth's rotation and is unrelated to luni-solar forcing.

Jason-1 GDRs do not explicitly provide values for the pure ocean tide, but instead provide values for a quantity referred to as the geocentric ocean tide, which is the sum total of the ocean tide and the load tide. Values of the load tide that were used to compute the geocentric ocean tide are also explicitly provided, so the pure ocean tide can be determined by subtracting the load tide value from the geocentric ocean tide value. Note that the permanent tide is not included in either the geocentric ocean tide or solid earth tide corrections that are provided on the Jason-1 GDRs.

5.9.1. Geocentric Ocean Tide

As mentioned above, the geocentric ocean tide is a quantity sometimes used to refer to the sum total of the ocean tide and the load tide. The Jason-1 GDR provides two choices for the geocentric ocean tide, ocean_tide_sol1 and ocean_tide_sol2, each of which is computed as the sum total of the diurnal and semidiurnal ocean and load tides as predicted by a particular model, and an equilibrium representation of the long-period ocean tides at all periods except for the zero frequency (constant) term. The two load tide values provided on the GDR, load_tide_sol1 and load_tide_sol2, provide the respective load tide values that were used to compute ocean_tide_sol1 and ocean_tide_sol2.

5.9.2. Long period Ocean Tide

The long-period ocean tides are a subject of continuing investigation. To first order, they can be approximated by an equilibrium representation. However, the true long-period ocean tide response is thought to have departures from an equilibrium response that increase with decreasing period. The two principal long-period ocean tide components, Mf and Mm, with fortnightly and monthly periods respectively, are known to have departures from an equilibrium response with magnitudes less than 1-2 cm.

The Jason-1 GDR explicitly provides a value for an equilibrium representation of the long-period ocean tide that includes all long-period tidal components excluding the permanent tide (zero frequency) component (see parameter ocean_tide_equil). Note that both geocentric ocean tide values on the GDR (ocean_tide_sol1 and ocean_tide_sol2) already include the equilibrium long-period ocean tide and should therefore not be used simultaneously.

The Jason-1 GDR provides a parameter for a non-equilibrium representation of the long-period ocean tides (see parameter ocean_tide_non_equil). This parameter is provided as a correction to the equilibrium long-period ocean tide model so that the total non-equilibrium long period ocean tide is formed as a sum of ocean_tide_equil and ocean_tide_non_equil.

5.9.3. Solid Earth Tide

The solid Earth responds to external gravitational forces similarly to the oceans. The response of the Earth is fast enough that it can be considered to be in equilibrium with the tide generating forces. Then, the surface is parallel with the equipotential surface, and the tide height is proportional to the potential. The two proportionality constants are the so-called Love numbers. It should be noted that the Love numbers are largely frequency independent, an exception occurs near a frequency corresponding to the K1 tide constituents due to a resonance in the liquid core [*Wahr*, 1985 and *Stacey*, 1977].

The Jason-1 GDR computes the solid earth tide, or body tide, as a purely radial elastic response of the solid Earth to the tidal potential (see parameter solid_earth_tide.) The adopted tidal potential is the *Cartwright and Tayler* [1971] and *Cartwright and Edden* [1973] tidal potential extrapolated to the 2000 era, and includes degree 2 and 3 coefficients of the tidal potential. The permanent tide (zero frequency) term is excluded from the tidal potential that is used to compute the solid earth tide parameter for the Jason-1 GDR. The elastic response is modeled using frequency independent Love numbers. The effects of the resonance in the core are accounted for by scaling the tide potential amplitude of the K1 tidal coefficient and some neighboring nodal terms by an appropriate scale factor.

5.9.4. Pole Tide

The pole tide is a tide-like motion of the ocean surface that is a response of both the solid Earth and the oceans to the centrifugal potential that is generated by small perturbations to the Earth's rotation axis. These perturbations primarily occur at periods of 433 days (called the Chandler wobble) and annual. These periods are long enough for the pole tide displacement to be considered to be in equilibrium with the forcing centrifugal potential. The Jason-1 GDR provides a single field for the radial geocentric pole tide displacement of the ocean surface (see pole_tide parameter), and includes the radial pole tide displacement of the solid Earth and the oceans.

The pole tide is easily computed as described in *Wahr* [1985]. Modeling the pole tide requires knowledge of proportionality constants, the so-called Love numbers, and a time series of perturbations to the Earth's rotation axis, a quantity that is now measured routinely with space techniques. Note that the pole tide on the IGDR and GDR may differ, since the pole tide on the GDR is computed with a more accurate time series of the Earth's rotation axis.

5.10. Inverse Barometer Effect

5.10.1. Inverted Barometer Correction

As atmospheric pressure increases and decreases, the sea surface tends to respond hydrostatically, falling or rising respectively. Generally, a 1-mbar increase in atmospheric pressure depresses the sea surface by about 1 cm. This effect is referred to as the inverse barometer (IB) effect.

The instantaneous IB effect on sea surface height in millimeters (see parameter inv_bar_corr) is computed from the surface atmospheric pressure, P_{atm} in mbar:

$$\text{inv\_bar\_corr} = -9.948 * (P_{atm} - P)$$

where P is the time varying mean of the global surface atmospheric pressure over the oceans.

The scale factor 9.948 is based on the empirical value [*Wunsch*, 1972] of the IB response at mid latitudes. Some researchers use other values. Note that the surface atmospheric pressure is also proportional to the dry tropospheric correction, and so the parameter inv_bar_corr approximately changes by 4 to 5 mm as model_dry_tropo_corr changes by 1 mm (assuming a constant mean global surface pressure). The uncertainty of the ECMWF atmospheric pressure products is somewhat dependent on location. Typical errors vary from 1 mbar in the northern Atlantic Ocean to a few mbars in the southern Pacific Ocean. A 1-mbar error in pressure translates into a 10 mm error in the computation of the IB effect.

Note that the time varying mean global pressure over the oceans, P, during the first eight years of the T/P mission had a mean value of approximately 1010.9 mbar, with an annual variation around this mean of approximately 0.6 mbar. However, the T/P data products provided a static inverse barometer correction referenced to a constant mean pressure of 1013.3 mbar.

$$IB(T/P) = -9.948 * (P_{atm} - 1013.3)$$

Sea surface heights that are generated after applying an inverse barometer correction referenced to a mean pressure of 1013.3 mbar are therefore approximately -9.948*(1010.9-1013.3) = 23.9 mm lower than those that are generated after applying an inverse barometer correction referenced to a time varying global mean pressure, and the difference between the two sea surface heights has an annual variation of approximately 9.948*0.6 = 6 mm.

5.10.2. Barotropic/Baroclinic Response to Atmospheric Forcing

The High Frequency Wind and Pressure Response correction, hf_fluctuations_corr, complements the Inverted Barometer (IB) correction. Like both tides and IB, the ocean response to wind and pressure (after removing the IB part) has energy at periods shorter than the 20 day implied by the ~10 day repeat cycle of Jason-1. This correction can be thought of as a departure from the IB response to pressure, although strictly it is the difference between the response to wind and pressure minus the IB. *Ali and Zlotnicki* [2000] compute this response with a barotropic model that is forced by NCEP operational wind and pressure. The model output is filtered in time to pass frequencies shorter than 20 days. See also *Stammer et al*. [2000] and *Tierney et al*. [2000].

The parameter hf_fluctuations_corr (and hf_fluctuations_corr_era) is provided in the GDR products as a correction to the inverse barometer correction inv_bar_corr (and inv_bar_corr_era).

5.11. Sigma 0 and Atmospheric Attenuation

The backscatter coefficients, sigma0 Ku and C values (see parameters sig0_ku and sig0_c), reported on the GDR are corrected for atmospheric attenuation using atmos_corr_sig0_ku and atmos_corr_sig0_c. Note that "unbiased" sigma0 values are recorded on the Jason-1 data products. For some geophysical algorithms, an appropriate bias is applied to the provided sigma0.

For defaulted atmospheric attenuation correction given by radiometer, a value of atmospheric attenuation correction has been calculated using the following formula:

atmos_corr_sig0_c = 2 x (Att_Sigma0_C_Coef[0] - Att_Sigma0_C_Coef[1] x model_wet_tropo_corr

atmos_corr_sig0_Ku = 2 x (Att_Sigma0_Ku_Coef[0] - Att_Sigma0_Ku_Coef[1] x model_wet_tropo_corr

Where att_sigma0_C_Coef[0] = 0.430e-1 dB

att_sigma0_C_Coef[1] = 0.783e-2 dB/meter

att_sigma0_Ku_Coef[0] = 0.594e-1 dB

att_sigma0_Ku_Coef[1] = 0.227e0 dB/meter

5.12. Wind Speed

The model functions developed to date for altimeter wind speed have all been purely empirical. A wind speed is calculated through a mathematical relationship with the Ku-band backscatter coefficient (corrected from atmospheric attenuation) and the significant wave height (see wind_speed_alt) using the Gourrion algorithm [*Gourrion et al*, 2002] and Collard table [*Collard*, 2005]. The wind speed model function is evaluated for 10 meter above the sea surface, and is considered to be accurate to 2 m/s.

A radiometer derived wind speed is also computed through an empirical relationship to brightness temperatures measured by the JMR [*Keihm et al.*, 1995] (see wind_speed_rad). The coefficients of this relationship have been determined from the regression of island radiosonde data computations combined with seasonal and latitude dependent wind speed statistics.

Finally, a 10-meter (above surface) wind vector (in east-west and north-south directions) is also provided on the Jason-1 GDR (see parameters wind_speed_model_u and wind_speed_model_v and wind_speed_model_u_era and wind_speed_model_v_era). This wind speed vector is determined from an interpolation of the ECMWF model (MARS 3D and ERA_interim data). The best accuracy for the wind vector varies from about 2 m/s in magnitude and 20 degrees in direction in the northern Atlantic Ocean, to more then 5 m/s and 40 degrees in the southern Pacific Ocean.

5.13. Bathymetry Information

The Jason-1 GDR provides a parameter bathymetry that gives the ocean depth or land elevation of the data point. Ocean depths have negative values, and land elevations have positive values. This parameter is given to allow users to make their own "cut" for ocean depth.

6. Data description

The main characteristics of Jason-1 level-2 products are summarized in the following table. During mission operations, three product families (OSDR, IGDR, and GDR) were available, and were provided in versions “a”, “b”, and “c”. All of those data are now superceded by the GDR version “e” product described in this handbook. Prior versions of this handbook provide more information about the OSDRs and IGDRs and their differences with respect to the GDR.

6.1. Data format

Accounting for Jason-1 heritage, the GDR version “e” products are split into three data sets:

- “SSHA” data set : One file SSHA, limited to 1Hz sampling values
- “GDR” data set : One file GDR, containing 1Hz and 20Hz values
- “SGDR” data set : One file SGDR, containing 1Hz, 20hz and waveforms values

6.1.1. NetCdf format and CF convention

The netCDF data format has been chosen to store the different data sets (one file per data set). This format is extremely flexible, self-documenting and has been adopted as a de-facto standard for many operational oceanography systems. What’s more, the files follow the Climate and Forecast NetCDF conventions CF-1.1 because these conventions provide a practical standard for storing.

6.1.2. The NetCDF Data Model

A netCDF file contains **dimensions**, **variables**, and **attributes**, which all have both a name by which they are identified. These components can be used together to capture the meaning of data and relations among data fields in an array-oriented data set.

6.1.2.1. Dimensions

A dimension may be used to represent a real physical dimension, for example, time, latitude, longitude, or height. A dimension might also be used to index other quantities (waveforms index for example). The following dimensions are used in the Jason-1 product files:

Dimension Name	Value	SSHA Data Set	GDR Data Set	SGDR Data Set
time	Number of measurements in the file	X	X	X
meas_ind	**20** (number of elementary measurements)		X	X
wvf_ind	**104** (number of waveform samples)			X

Table 17 - Dimensions used in the Jason-1 data sets

6.1.2.2. Variables

Variables are used to store the bulk of the data in a netCDF file. A variable represents an array of values of the same type. A scalar value is treated as a 0-dimensional array. A variable has a name, a data type, and a shape described by its list of dimensions specified when the variable is created. A variable may also have associated attributes, which may be added, deleted or changed after the variable is created.

A variable data type is one of a small set of netCDF types. In this document the variable types will be represent as follows:

Variable type	Description

char	characters
byte	8-bit data signed
short	16-bit signed integer
int	32-bit signed integer
float	IEEE single precision floating point (32 bits)
double	IEEE double precision floating point (64 bits)

Table 18 - netCDF variable type

6.1.2.3. Coordinate variables and auxiliary coordinate variables

A variable with the same name as a dimension is called a **coordinate variable**. It typically defines a physical coordinate corresponding to that dimension. In accordance with the Climate and Forecast conventions, we must declare a coordinate variable for each dimension. What's more, missing values are not allowed in coordinate variables and they must be strictly monotonic.

An **auxiliary coordinate variable** is a netCDF variable that contains coordinates data but is not a coordinate variable as defined above. Unlike coordinate variables, there is no relationship between the name of an auxiliary coordinate variable and the name(s) of its dimension(s).

6.1.2.4. Attributes

NetCDF attributes are used to store data about the data (ancillary data or metadata), similar in many ways to the information stored in data dictionaries and schema in conventional database systems. Most attributes provide information about a specific variable. These are identified by the name of that variable, together with the name of the attribute.

Some attributes provide information about the data set as a whole. They are called **global attributes** - similar to the header of the Jason-1 products.

The following table shows the variable attributes used in the Jason-1 product. There are no mandatory attributes.

Attribute	Description
_FillValue	A default value used to represent missing or undefined data
add_offset	If present, this number is to be added to the data after it is read by an application. If both *scale_factor* and *add_offset* attributes are present, the data are first scaled before the offset is added
calendar	Reference time calendar
comment	Miscellaneous information about the data or the methods used to produce it
coordinates	Identified auxiliary coordinates variables
flag_meanings	Use in conjunction with *flag_values* to provide descriptive words or phrase for each flag value
flag_values	Provide a list of the flag values. Use in conjunction with *flag_meanings*
institution	Institution which provides the data
leap_second	UTC time at which a leap second occurs
long_name	A descriptive name that indicates a variable's content. This name is not standardized
quality_flag	Name of the variable(s) (quality flag) representing the quality of the current variable
scale_factor	If present, the data are to be multiplied by this factor after the data are read by an application. See also *add_offset* attribute
source	Data source (model features, or observation)
standard_name	A standard name that references a description of a variables content in the standard name table
tai_tuc_difference	Difference between TAI and UTC reference time
units	Unit of a variable's content. The value of this attribute must be a string that can be recognized by the UNIDATA's Udunits package
valid_max	Largest theoretical valid value of a variable (this is not the maximum of actual data)
valid_min	Smallest theoretical valid value of a variable (this is not the minimum of actual data)

Table 19 - Variable's attributes

6.1.3. The Common Data Language

The Common Data Language (CDL) is used to describe the content of a data set.

The CDL is textual notation that described the netCDF object and it is human readable. The netCDF utility **ncdump** converts netCDF objects binary to CDL text. The netCDF utility **ncgen** creates netCDF binary file from CDL text file.

A CDL description of a netCDF data set takes the form:

```
netCDF name {
dimension: …
variables: …
data: …
}
```

where the name is used only as a default in constructing file names by the ncgen utility. The CDL description consists of three optional parts, introduced by the keywords dimensions variables and data. NetCDF dimension declarations appear after the dimensions keyword, netCDF variables and attributes are defined after the variables keyword and variable data assignments appears after the data keyword. CDL statement are terminated by a semicolon. Spaces, tabs and newlines can be used freely for readability. Comments in CDL follow the characters '//' on any line.

<u>Example</u>

```
netcdf example {
 dimensions:                              //  dimensions name are declared first
  time = 2680;

  variables:
  double time(time);                      // variable <type> <name>(<dimension>)
     time:long_name = "time";             // variable attributes
     time:units = "seconds since 2000-01-01 00:00:00.0";

  int lon(time);
     lon:long_name = "longitude";
     lon:standard_name = "longitude";
     lon:units = "degrees_east";
     lon:scale_factor = 1.0e-06;

  byte alt_echo_type(time);
     alt_echo_type:long_name = "altimeter echo type";
     alt_echo_type:_FillValue = 127b;
     alt_echo_type:flag_values = 0b, 1b ;
     alt_echo_type:flag_meanings = "ocean_like non_ocean_like";
     alt_echo_type:coordinates = "lon lat";

   int alt(time);
     alt:long_name = "1 Hz altitude of satellite";
     alt:_FillValue = 2147483647;
     alt:units = "m";
     alt:add_offset = 1.30e+06;
     alt:scale_factor = 1.00e-04;
     alt:coordinates = "lon lat";
```

- time is a coordinate variable
- alt_echo_type is a flag fully described by the flag_meanings and flag_values attributes:

  alt_echo_type = 0 -> ocean like echo
  alt_echo_type = 1 -> non ocean like echo

If alt_echo_type is not computed, it will take the value 127 (_FillValue attribute).

- alt is packed. The data are stored in 32-bit integers (long). The value of the altitude of the satellite can be recovered using:

  $alt = (alt_{long} * scale\_factor) + add\_offset$

6.2. Global attributes

Global attributes (the equivalent of header parameters for Jason-1 products) may be displayed from a SSHA/GDR/SGDR data set file using **"ncdump -h"** command.

A list (not necessarily exhaustive) of the global attributes available in these data sets is given below (attribute name and description).

Conventions	netCDF convention followed
title	A descriptive title for the data set
institution	The name of the data producer
source	The method of production of original data
history	Date and Product Create Time
contact	A text giving the primary contact for information about the data set
references	The version of the altimetric library used to produce the data set
processing_center	Name of the processing center
reference_document	Name of the reference document describing the products
mission_name	Name of the mission
altimeter_sensor_name	Name of the altimeter sensor
radiometer_sensor_name	Name of the radiometer sensor
doris_sensor_name	Name of the DORIS sensor
acq_station_name	Identification of the acquisition station
cycle_number	Cycle number
absolute_rev_number	Absolute number of revolution
pass_number	Pass number in the cycle (relative pass number)
absolute_pass_number	Absolute pass number (since the beginning of the mission)
equator_time	UTC time of equator crossing
equator_longitude	Longitude of equator crossing
first_meas_time	First measurement time
last_meas_time	Last measurement time
ellipsoid_axis	Semi-major axis of the reference ellipsoid
ellipsoid_flattening	Flattening coefficient of the reference ellipsoid

6.3. Data Sets

Variables attributes are identified in section 6.1.2.4 they may be displayed from a SSHA/GDR/SGDR data set file using **"ncdump -h"** command.

Some examples (not necessarily fully up to date) are given below:

```
double time(time=2450);
     :long_name = "time (sec. since 2000-01-01)";
     :standard_name = "time";
     :calendar = "gregorian";
     :tai_utc_difference = 32.0; // double
     :leap_second = "0000-00-00 00:00:00";
     :units = "seconds since 2000-01-01 00:00:00.0";
     :comment = "[tai_utc_difference] is the difference between TAI - UTC (i.e., leap seconds) for the first measurement of the data set. [leap_second] is the UTC time at which a leap second occurs in the data set, if any. After this UTC time, the [tai_utc_difference] is increased by 1 second. time variable is corrected from datation bias. See Jason-1 User handbook.";

   byte meas_ind(meas_ind=20);
     :long_name = "elementary measurement index";
     :units = "count";
     :comment = "Set to be compliant with the CF-1.1 convention";

   double time_20hz(time=2450, meas_ind=20);
     :_FillValue = 1.8446744073709552E19; // double
     :long_name = "time 20 Hz (sec. since 2000-01-01)";
     :standard_name = "time";
     :calendar = "gregorian";
     :tai_utc_difference = 32.0; // double
```

```
    :leap_second = "0000-00-00 00:00:00";
    :units = "seconds since 2000-01-01 00:00:00.0";
    :comment = "[tai_utc_difference] is the difference between TAI - UTC (i.e., leap seconds) for the first measurement of the data set. [leap_second] is the UTC time at which a leap second occurs in the data set, if any. After this UTC time, the [tai_utc_difference] is increased by 1 second. time_20hz variable is corrected from datation bias. See Jason-1 User handbook.";

  int lat(time=2450);
    :long_name = "latitude";
    :standard_name = "latitude";
    :units = "degrees_north";
    :quality_flag = "orb_state_flag_rest";
    :scale_factor = 1.0E-6; // double
    :comment = "Positive latitude is North latitude, negative latitude is South latitude. See Jason-1 User Handbook.";

  int lon(time=2450);
    :long_name = "longitude";
    :standard_name = "longitude";
    :units = "degrees_east";
    :quality_flag = "orb_state_flag_rest";
    :scale_factor = 1.0E-6; // double
    :comment = "East longitude relative to Greenwich meridian. See Jason-1 User Handbook.";

  int lon_20hz(time=2450, meas_ind=20);
    :_FillValue = 2147483647; // int
    :long_name = "20 Hz longitude";
    :standard_name = "longitude";
    :units = "degrees_east";
    :scale_factor = 1.0E-6; // double
    :comment = "East longitude relative to Greenwich meridian. See Jason-1 User Handbook";

  int lat_20hz(time=2450, meas_ind=20);
    :_FillValue = 2147483647; // int
    :long_name = "20 Hz latitude";
    :standard_name = "latitude";
    :units = "degrees_north";
    :scale_factor = 1.0E-6; // double
    :comment = "Positive latitude is North latitude, negative latitude is South latitude. See Jason-1 User Handbook";

  byte surface_type(time=2450);
    :_FillValue = 127B; // byte
    :long_name = "surface type";
    :flag_values = 0B, 1B, 2B, 3B; // byte
    :flag_meanings = "ocean lake_enclosed_sea ice land";
    :coordinates = "lon lat";
    :comment = "Computed using a DTM2000 file: 0 = open oceans or semi-enclosed seas; 1 = enclosed seas or lakes; 2 = continental ice; 3 = land. See Jason-1 User Handbook";


short ssha(time=2450);
    :_FillValue = 32767S; // short
    :long_name = "sea surface height anomaly";
    :standard_name = "sea_surface_height_above_sea_level";
    :source = "Poseidon-2";
    :institution = "CNES";
    :units = "m";
    :scale_factor = 0.001; // double
    :coordinates = "lon lat";
    :comment = "= altitude of satellite (alt) - Ku band corrected altimeter range (range_ku) - altimeter ionospheric correction on Ku band (iono_corr_alt_ku) - model dry tropospheric correction (model_dry_tropo_corr) - radiometer wet tropospheric correction (rad_wet_tropo_corr) - sea state bias correction in Ku band (sea_state_bias_ku) - solid earth tide height (solid_earth_tide) - geocentric ocean tide height solution 1 (ocean_tide_sol1) - geocentric pole tide height (pole_tide) - inverted barometer height correction (inv_bar_corr) - high frequency fluctuations of the sea surface topography (hf_fluctuations_corr for I/GDR off line products only) - mean sea surface (mean_sea_surface). Set to default if the altimeter echo type (alt_echo_type) is set to 1 = non ocean like, the radiometer surface type (rad_surf_type) set to 2 = land, or the rain flag (rain_flag) set to 1 = rain";
```

6.4. Software

This section lists some software that may be used to browse and use data from SSHA, GDR and SGDR data sets.

6.4.1. Software provided with netCDF : “ncdump”

« ncdump » converts netCDF files to ASCII form (CDL)

See http://www.unidata.ucar.edu/software/netcdf/docs/ncdump-man-1.html

The main options are the following:

-h	Show only the header information in the output that is the declarations of dimensions, variables, and attributes but no data values for any variables
-c	Show the values of coordinate variables (variables that are also dimensions) as well as the declarations of all dimensions, variables, and attribute values
-v *var1,...,varn*	The output will include data values for the specified variables, in addition to the declarations of all dimensions, variables, and attributes
-x *var1,...,varn*	Output XML (NcML) instead of CDL. The NcML does not include data values

6.4.2. Additional general software

6.4.2.1. ncbrowse

“ncBrowse” is a Java application that provides flexible, interactive graphical displays of data and attributes from a wide range of netCDF data file conventions.

See http://www.epic.noaa.gov/java/ncBrowse/

6.4.2.2. netCDF Operator (NCO)

The netCDF Operators, or “NCO”, are a suite of programs known as **operators**. Each operator is a standalone, command line program which is executed at the UNIX shell-level, like, e.g., `ls` or `mkdir`. The operators take netCDF files as input, then perform a set of operations (e.g., deriving new data, averaging, hyperslabbing, or metadata manipulation) and produce a netCDF file as output. The operators are primarily designed to aid manipulation and analysis of gridded scientific data. The single command style of NCO allows users to manipulate and analyze files interactively and with simple scripts, avoiding the overhead (and some of the power) of a higher level programming environment.

See http://nco.sourceforge.net/

6.4.3. Additional specific software : “BRAT”

The “Basic Radar Altimetry Toolbox” is a collection of tools and tutorial documents designed to facilitate the use of radar altimetry data. It is able to read most distributed radar altimetry data from all the satellites, to do some processing, data editing and statistic over them, and to visualize the results. The Basic Radar Altimetry Toolbox is able to read ERS-1 and 2, TOPEX/Poseidon, GEOSAT Follow-on, Jason-1, ENVISAT, Jason-1 and CRYOSAT missions altimetry data from official data centers (ESA, NASA/JPL, CNES/AVISO, NOAA), and this for different processing levels, from level 1B (Sensor Geophysical Data Record) to level 3/4 (gridded merged data).

See http://www.altimetry.info/html/data/toolbox_en.html

Annexe A - References

Ali, A. H., and V. Zlotnicki (2003), Quality of wind stress fields measured by the skill of a barotropic ocean model: Importance of stability of the Marine Atmospheric Boundary Layer, *Geophys. Res. Lett.*, 30(3), 1129, doi: 10.1029/2002GL016058.

Bonnefond, P., P. Exertier, O. Laurain, Y. Menard, A. Orsoni, E. Jeansou and G. Jan, 2002, "Absolute calibration of Jason-1 and TOPEX/POSEIDON altimeters in Corsica (abstract)", Jason-1/TOPEX/POSEIDON Science Working Team, New Orleans, LA, USA.

Brenner, A. C., C. J. Koblinsky, and B. D. Beckley, 1990, A Preliminary Estimate of Geoid-Induced Variations in Repeat Orbit Satellite Altimeter Observations, *J. Geophys. Res.*, 95(c3), 3033-3040.

Brown, S., 2009, A Novel Near-Land Radiometer Wet Path Delay Retrieval Algorithm: Application to the Jason-2/OSTM Advanced Microwave Radiometer", submitted to IEEE Trans. Geosci. Rem. Sens.

Callahan, P. S., 1984, Ionospheric Variations affecting Altimeter Measurements: A brief synopsis *Marine Geodesy*, 8, 249-263.

Carrere, L., F. Lyard, M. Cancet, and A. Guillot (2015), FES2014, a new tidal model on global ocean with enhanced accuracy in shallow seas and Arctic region, European Geophysical Union meeting.

Cartwright, D. E. and R. J. Tayler, 1971, New computations of the tide-generating potential, *Geophys. J. R. Astr. Soc.*, 23, 45-74.

Cartwright, D. E. and A. C. Edden, 1973, Corrected tables of tidal harmonics, *Geophys. J. R. Astr. Soc.*, 33, 253-264.

Chelton, D. B., J. C. Ries, B. J. Haines, L. L. Fu, and P. S. Callahan, 2001, "Satellite Altimetry", *Satellite Altimetry and Earth Sciences*, ed. L.L. Fu and A. Cazenave, pp. 1-131.

Collard, F., 2005, Algorithmes de vent et periode moyenne des vagues JASON a base de reseaux de neurons, BO-021-CLS-0407-RF, Boost Technologies, 33pp.

Cruz Pol, S. L., C. S. Ruf, and S. J. Keihm, 1998, Improved 20-32 GHz atmospheric absorption model, *Radio Science*.

Desai, S. D. (2002), Observing the pole tide with satellite altimetry, *J. Geophys. Res.*, 107 (C11), doi:10.1029/2001JC001224.

Desai, S. D., and R. D. Ray (2014), Consideration of tidal variations in the geocenter on satellite altimeter observations of ocean tides, *Geophys. Res. Lett.*, 41, 2454-2459, doi:10.1002/2014GL059614.

Gourrion, J., D. Vandemark, S. Bailey, B. Chapron, G. P. Gommenginger, P. G. Challenor, and M. A. Srokosz, A two-parameter wind speed algorithm for Ku-Band altimeters, *J. Atmos. and Oceanic Tech.*, 19, 2030-2048.

Haines, B., D. Kubitschek, G. Born and S. Gill, 2002, "Monitoring Jason-1 and TOPEX/POSEIDON from an offshore platform: The Harvest experiment (abstract)", Jason-1/TOPEX/POSEIDON Science Working Team, New Orleans, LA, USA.

Imel, D., 1994, Evaluation of the TOPEX dual-frequency Ionosphere correction, *J. Geophys. Res.*, 99 (c12), pp 24895-24906.

Keihm, S. J., M. A. Janssen, and C. S. Ruf, 1995, TOPEX/POSEIDON microwave radiometer (TMR): III. Wet troposphere range correction algorithm and pre-launch error budget, *IEEE Trans. Geosci. Remote Sensing*, 33, 147-161.

Le Provost, C., 2001, "Ocean Tides", *Satellite Altimetry and Earth Sciences*, ed. L.L. Fu and A. Cazenave, pp. 267-303.

Le Provost, C., F. Lyard, M. L. Genco, F. Lyard, P. Vincent, and P. Canceil, 1995, Spectroscopy of the world ocean tides from a finite element hydrodynamic model, *J. Geophys. Res.*, 99, 24777-24797.

Lemoine, F. G. et al., 1998, The Development of the joint NASA GSFC and NIMA Geopotential Model EGM96, NASA/TP-1998-206861, 575 pp.

Pavlis, N. and R. H. Rapp, 1990, The development of an isostatic gravitational model to degree 360 and its use in global gravity modeling, *Geophys. J. Int.*, 100, 369-378.

Ray, R. D., 2013, Precise comparisons of bottom-pressure and altimetric ocean tides, *J. Geophys. Res. Oceans*, 118, 4570-4584, doi:10.1002/jgrc.20336.

Ray, R.D., and R. M. Ponte (2003), Barometric tides from ECMWF operational analyses, *Annales Geophysicae*, 21, 1897-1920.

Rodriguez, E., Y. Kim, and J. M. Martin, 1992, The effect of small-wave modulation on the electromagnetic bias, *J. Geophys. Res.*, 97(C2), 2379-2389.

Ruf, C., S. Keihm, B. Subramanya, and M. Janssen, 1994, TOPEX/POSEIDON microwave radiometer performance and in-flight calibration, *J. Geophys. Res.*, 99, 24915-24926.

Smith, W. H. F. and D. T. Sandwell, 1994, Bathymetric prediction from dense satellite altimetry and spare shipboard bathymetry, *J. Geophys. Res.*, 99, 21803-21824.

Stacey, F. D., 1977, *Physics of the Earth*, second ed. J. Wiley, 414 pp.

Stammer, D., C. Wunsch, and R. M. Ponte, 2000, De-aliasing of global high frequency barotropic motions in altimeter observations, *Geophys. Res. Lett.*, 27, 1175-1178.

Tierney, C., J. Wahr, F. Bryan, and V. Zlotnicki, 2000, Short-period oceanic circulation: implications for satellite altimetry, *Geophys. Res. Lett.*, 27, 1255-1258.

Tournadre, J., and J. C. Morland, 1998, The effects of rain on TOPEX/POSEIDON altimeter data, *IEEE Trans. Geosci. Remote Sensing*, 35, 1117-1135.

Tran, N., P. Thibaut, J.-C. Poisson, S. Philipps, E. Bronner, and N. Picot (2011), Impact of Jason-2 wind speed calibration on the sea state bias correction, *Marine Geodesy*, 34, 407-419, doi:10.1080/01490419.2011.584832.

Wahr, J. M. (1985), Deformation induced by polar motion, *J. Geophys. Res.*, 90 (B11), 9363-9368, doi: 10.1029/JB090iB11p09363.

Wunsch, C., 1972, Bermuda sea level in relation to tides, weather and baroclinic fluctuations, *Rev. Geophys. Space Phys.*, 10, 1-49.

Annexe B - List of acronyms

AD	Applicable Document
AGC	Automatic Gain Control
AMR	Advanced Microwave Radiometer
AVISO	Archivage, Validation et Interprétation des données des Satellites Océanographiques
BRAT	Basic Radar Altimetry Toolbox
CLIVAR	Climate Variability and Predictability program
CLS	Collecte Localisation Satellites
CNES	Centre National d'Etudes Spatiales
DIODE	Détermination Immédiate d'Orbite par Doris Embarque
DORIS	Détermination d'Orbite et Radiopositionnement Intégrés par Satellite
DTM	Digital Terrain Model
ECMWF	European Center for Medium range Weather Forecasting
EGM	Earth Gravity Model
EM	ElectroMagnetic
EUMETSAT	European Organisation for the Exploitation of Meteorological Satellites
FES	Finite Element Solution
FFT	Fast Fourier Transform
GDR	Geophysical Data Records
GIM	Global Ionosphere Maps
GODAE	Global Ocean Data Assimilation Experiment
GPS	Global Positioning System
GTS	Global Telecommunications System
HF	High Frequency
IB	Inverse Barometer
IGDR	Interim Geophysical Data Records
JGM	Joint Gravity Model
JMR	JMR Jason-1 Microwave Radiometer
JPL	Jet Propulsion Laboratory
LPT	Light Particle Telescope
MDT	Mean Dynamic Topography
MLE	Maximum Likelihood Estimator
MSS	Mean Sea Surface
NASA	National Aeronautics and Space Administration
NetCDF	Network Common Data Form
NRT	Near Real Time
NWP	Numerical Weather Prediction
OSDR	Operational Geophysical Data Records
OSTM	Ocean Surface Topography Mission
OSU	Ohio State University
PO.DAAC	Physical Oceanography Distributed Active Archive Center
POD	Precision Orbit Determination
POE	Precision Orbit Ephemerides
PROTEUS	Plateforme Reconfigurable pour l'Observation de la Terre, les télécommunications et les Utilisations Scientifiques
RD	Reference Document
RMS	Root Mean Square
RSS	Root Sum Square
SLA	Sea Level Anomaly
SLR	Satellite Laser Ranging
SSALTO	Segment Sol multimissions d'ALTimétrie, d'Orbitographie et de localisation précise
SSB	Sea State Bias
SSH	Sea Surface Height
SSHA	Sea Surface Height Anomaly
SWH	Significant Wave Height
T/P	Topex/Poseidon
TBC	To be confirmed

TBD	To be defined
TEC	Total Electron Content
TRSR	Turbo Rogue Space Receiver
UTC	Universal Time Coordinated
WMO	World Meteorological Organisation

Annexe C - Contacts

CNES

18, avenue Edouard Belin
F-31401 Toulouse Cedex 9

Web : www.cnes.fr

AVISO+ User Service Helpdesk:

8-10 rue Hermès
F-31520 Ramonville-St-Agne, France

Phone : +33 (0) 5 61 39 47 80
Fax : +33 (0) 5 61 39 37 82
Web : www.aviso.altimetry.fr
e-mail : aviso@altimetry.fr

NASA

Web : http://www.nasa.gov/

PO.DAAC User Services:

Jet Propulsion Laboratory
MS T1721-202
4800 Oak Grove Drive
Pasadena, CA 91109 USA

Phone : +1 818-393-7165
Fax : +1 818-393-3405
Web : http://podaac.jpl.nasa.gov
e-mail : podaac@podaac.jpl.nasa.gov